ACS OMEGA

http://pubs.acs.org/journal/acsodf

Article

Research on the Dynamic Response Properties of Nonlethal Projectiles for Injury Risk Assessment

Noureddine Boumdouha,* Jannick Duchet-Rumeau, Jean-François Gerard, Djalel Eddine Tria, and Amar Oukara

Cite This: *ACS Omega* 2022, 7, 47129−47147

Read Online

ACCESS | Metrics & More | Article Recommendations | Supporting Information

ABSTRACT: Based on the models already on the market, we have manufactured six types of nonlethal projectiles. We have made convex heads out of polyurethane foam (PUR) filled with mineral fillers like alumina (Al_2O_3) and montmorillonite (MMT). We chose a suitable holder for nonlethal projectiles. Also, we made a custom industrial model and used CAD modeling in SolidWorks to simulate the deformation of the nonlethal projectiles. The polymeric nonlethal projectile holders were then 3D-printed. We performed a dynamic mechanical analysis (DMA) and discussed the results. Likewise, we conducted ballistic impact experiments on nonlethal projectiles (XM1006) and nonlethal projectiles manufactured that were evaluated using a rigid wall and a pneumatic launcher. Furthermore, we looked at cell structure, the spread of the mean pore diameter, and the particle size distributions of the mineral fillers using scanning electron microscopy (SEM). We evaluated and discussed injury risks from nonlethal impacts. Data on nonlethal projectile lethality and safe impact speed are collected. This study explains how lab studies and real-world practice coexist through nonlethal projectile properties.

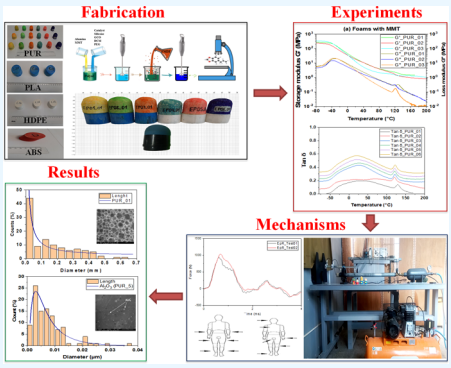

1. INTRODUCTION

Polyurethane foam, known as PUR foam, has evolved for years.[1] It can be graded as flexible foam and hardness-based foam.[2−4] Rigid PUR foam is used more than flexible foam. The rigid PUR foams have a closed-cell structure and promising applications containing improved thermal isolation,[5,6] lighter weight, greater resistance, and more experimental treatment.[7,8] Nanodispersions protection of carbon nanofiber for polyurethane foaming,[9,10] thermal protection,[11,12] impact buffering,[13−15] etc. Thus, to expand its applications, making its interdisciplinary polyurethane foam is now a trend.[16−18]

The commercial use of polymer foam is increasing and is instrumental in shock applications, thermal and acoustic insulation, and filters. They are used in the aircraft, aerospace, building, and packaging industries.[19,20] Rigid polyurethane foams that combine mechanical solid aptitude and low-density properties can be used as material structural.[21] Regardless of their application, their optimization must consider the relationship between microstructure and mechanical properties.[22] Indeed, their automatic response depends on the content architecture and the polymer's intrinsic characteristics in the cell wall.[23] The structure depends on the cell wall size, distribution of cell size, and cell form.

Nonlethal kinetic energy weapons stop people from doing dangerous or illegal things without hurting them for good. Nonlethal projectiles are employed to incapacitate and neutralize individuals during riots, crowd control, and apprehend suspicious naval vessels.[24] They provide an option for an adequate reaction by ensuring neutralization without causing irreversible harm to the targeted individuals. There is a vast selection of products. Nevertheless, the study focuses on characterizing different degrees of polyurethane foam. Numerous incidents of major injuries produced by this nonlethal projectile have been reported.[25]

Consequently, it is vital to link the manufacturing process with the product by assessing the lesion risk of these projectiles. Assessing the lesion risk is an excellent idea for developing safer projectiles.[26] Multiple materials are employed to ensure the gentle usage of nonlethal projectile weapons, modified polyurethane foam being the most common.[27] Biomechanical aspects are used to study the impact of head injuries resulting from the breach, where the head injury depends on linear acceleration to assess infection.[28]

The 1999 North Atlantic Treaty Organization's NATO policy's meaning of nonlethal weapons (NLW) has remained a point of reference for any essential appraisal of them: they were labeled as "Nonlethal arms which are explicitly designed and developed to incapacitate or repel personnel, with a low probability of fatality or permanent injury, or to disable

Received: September 28, 2022
Accepted: November 25, 2022
Published: December 8, 2022

Table 1. Mineral Fillers Used for Their Physicochemical Properties

mineral fillers	density (g/cm^3)	average diameter (μm)	poisson coefficient	specific surfaces (m^2/g)	modulus (GPa)
alumina (Al_2O_3)	3.95	0.009	0.21	3.2	215
montmorillonite (MMT)	1.9 to 2.7	0.1	0.4	14.908	178

Table 2. Essential Compounds in the Preparation of Polyurethane Foam

	A						B		C
polyurethane foam	polyol POPE (wt %)[a]	silicone L-580 (wt %)[b]	glycerol GCO (wt %)[c]	dichloromethane DCM (wt %)[d]	catalyst A-33 (wt %)[e]	polyethylene glycol PEG (wt %)[f]	alumina Al_2O_3 (wt %)[g]	montmorillonite MMT (wt %)[h]	polymeric diphenylmethane diisocyanate PMDI (wt %)[i]
PUR_01	62.58	0.83	1.38	0.74	0.93	0.5	0	3	30.04
PUR_02	59.09	2.07	2.19	0.28	1.26	0.25	0	6	28.86
PUR_03	58.44	1.46	2.15	0.26	1.26	0.18	0	9	27.25
PUR_04	62.17	1.54	2.29	0.38	1.04	1.24	3	0	28.34
PUR_05	58.83	1.24	2.28	1.24	1.79	1.23	6	0	27.39
PUR_06	65.94	2.75	1.01	0.82	1.76	1.11	9	0	17.61

[a]POPE (3500 g·mol^{-1}; 10% SAN; $I_{OH=}$43 mg KOH/g; density/viscosity = 1023/895 mPa.s). [b]L-580 (112.17 g·mol^{-1}; 1.026 density at 25 °C; 1000 viscosity at 25 °C). [c]GCO (92.10 g·mol^{-1}; 32.57 OH / kg). [d]DCM (84.93 g·mol^{-1}). [e]A-33 (112.17 g·mol^{-1}; 33% in dipropylene glycol). [f]PEG (44.05 g·mol^{-1}). [g]Al_2O_3 (101.96 g·mol^{-1}). [h]MMT (218.09 g·mol^{-1}). [i]PMDI (250.25 g·mol^{-1}; 31%NCO; density/viscosity = 1.02/337 mPa.s).

equipment, with minimal undesired damage or impact on the environment."[29] This article aims to give society real-world examples of nonlethal kinetic energy usage (NLW).[30] Potential injuries and efficacy are the key areas of concern. The methodology is multidisciplinary since the operational, medical, and projectile dimensions reflect significant facets of a consistent analysis. Given the production and implementation of criteria, real-world outcomes may be linked to conventional forecasts.[31]

Nonlethal arms (NLW) enable police and military forces to react more effectively and are less likely to escalate aggression and noncompliance by opponents.[32] Specifically, preventing civilian casualties supports the "hearts and minds" approach at the political and strategic levels.[33,34] Pain that is expected is often associated with the term "performance." However, the related projectile or medical literature is weak, providing details on the usage and results of these nonpenetrative projectiles that disable or repel individuals by inducing discomfort in general. Some scholars speak about direct projectile effects. At their destination, warheads are shot comparatively low, thereby restricting the maximum risk to humans. Accidents have, however, occurred where NLW-induced (Permanent) skin injury. Because of this, there needs to be a way to keep nonlethal projectiles from penetrating the skin.

A NATO standard[35] connects the projectile's most contact surface with the target and utilizes its ordinary tension ratio to calculate the system's effect on the human corpse; it should not exceed the maximum MPa. Recent efforts to provide a uniform method for evaluating nonlethal arms impact have been fruitful and made through NATO Recommendation for Standardization (STANREC).[36] STANTEC offers testing procedures that take round accuracy,[37] penetration risk, and the effect of blunt force.[38] Therefore, to thoroughly examine the 40 MM impact munitions' human consequences, fundamental design characterization and evaluation of injury risk procedures were used.

The resistance to the impact of nonlethal projectiles is being studied.

The resistance to the impact of nonlethal projectiles is being studied. They generally adopt shock absorption designs and unique structures to reduce damage to humans[39] and absorb energy and stress. Thus, this study modified its good and strengthening type and content to strengthen the mechanical properties of PUR foam by adding additives. In pneumatic launcher tests, resilience rates, bursting, and dynamic punch strength will then be examined for properties of the nonlethal projectile by polyurethane foam enhanced.

The efficiency of less damaging weapon structures has not yet been formalized by scientists when force is utilized, despite a rich scholarly literature on police usage. According to recent research, most experts have focused on racial violence, excessive force, and corpse exploitation.[40] They illustrate the distinction between death and a nonlethal force that would be eligible for power over a person but does not destroy or seriously injure it. They deal with the light, nonlethal control of what is considered socially permissible. According to the products of the measurement tools in this study, because the nonlethal projectiles created have pressure and impact strength effective, they are more efficient and effective for commercialization. This research can evaluate the risk of injury from these impacts, and the limitations of current work can be applied to mitigate the dangers associated with nonlethal projectile weapons.

2. EXPERIMENTAL SECTION

2.1. Materials and Methods. Confortchem supplied the commercial polyester polyol STEPANPOPE PS-2352 and the aromatic diisocyanate PUROCYN B. Niax offered the silicone surfactant TEGOSTAB B8513 and the PUR metal catalyst triethylenediamine (A-33). AcroSeal supplied dichloromethane (blowing agent). Saidal showed glycerol (GCO), hydrochloric acid (99.9%), ethanol (99.9%), and sulfuric acid (95%). Mineral fillers alumina (Al_2O_3) and montmorillonite (MMT) are provided by the Bental company. We purchased mineral fillers based on physical and chemical qualities, as seen in Table 1.

Alumina and MMT fillers were steeped in NaOH solution (10%) for 1 h. After that, 1% acetic acid was used to neutralize it. Finally, the stuffing was rinsed with pH seven ultrapure water and baked for 24 h at 80 °C. The fillers have good

https://doi.org/10.1021/acsomega.2c06265
ACS Omega 2022, 7, 47129−47147

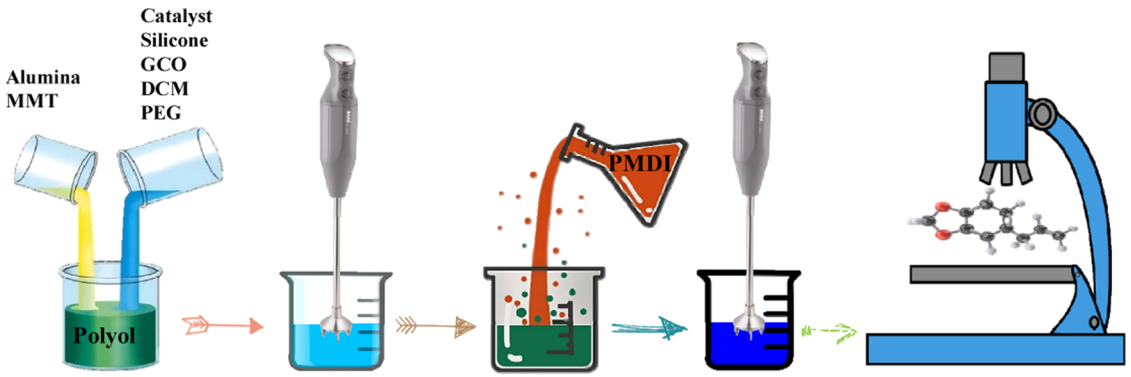

Figure 1. Procedural schematic for the preparation of polyurethane foams.

Figure 2. General appearance of dynamic testable samples: (a) Six optimized formulas of nonlethal projectiles in polyurethane foam; (b) Samples of natural beechwood; c. Samples made of artificial plywood; d. Samples of nonlethal projectile holders made of acid polylactic (PLA); e. Samples of nonlethal projectile holders made of acrylonitrile butadiene styrene (ABS); f. Samples of nonlethal projectile holders made of high-density polyethylene (HDPE).

properties, especially alumina, which has an average diameter of 0.009 μm, compared to 0.1 μm of MMT, which will be distributed uniformly on the surface of the polyurethane foam cells.

2.2. Elaboration of Polyurethane Foams (PUR). A preliminary study let us choose the six most promising polyurethane foams, specially prepared to suit the application of nonlethal projectiles. We summarize the preparation methods used in preparing these samples. The elements of the polymer matrix are mixed for 30 s at 2500 rpm using a (Rainy) mixer with circling blades. The mixture is blended for 15 seconds at 2500 rpm and poured into a cylindrical mold. Foams are formed by free (24 h) expansion of the mold. After the preparation, we perform the mechanical and microscopic

https://doi.org/10.1021/acsomega.2c06265
ACS Omega 2022, 7, 47129−47147

characterization to adjust these formulas according to nonlethal ballistics requirements. Due to the sensitivity of the promoted goal, we have been keen on harnessing all available resources to achieve a satisfactory result. Table 2 summarizes the characteristics of these candidates.

PUR is developed in a free expansion mode and poured into a unique Teflon flask, where the foam cell begins to form. The additives and catalysts used in this process are assisted after reaching the appropriate foam for our application. The foam leaves atmospheric pressure to take its final shape. After the polyurethane is thickened and cooled, it is removed from the mold, resulting in a foam having Figure S1 in the Supporting Information. The diagram in Figure 1 summarizes how the preparation of polyurethane foam.

ISO 2555 was used to determine PUR systems' viscosity.[41] Measurement was taken using a DVII rotatory viscometer. The PUR systems viscosity was measured at varying sharing rates of 10, 20, 30, and 100 rpm (round per minute). A total of six individual measurements were analyzed, and we computed the standard deviation.

2.3. Preparing Nonlethal Projectiles. We designed the nonlethal projectile head to dissipate energy when hitting the target, using the raw materials available in the market to produce the lowest cost and breakable polyurethane foam compressible to reduce the impact force. We designed the mount as a base for projectiles using the dimensions of commercially accessible designs. We studied the strength of some wood and polymeric materials and found that the polymer, with its enhanced properties, helps reduce the possibility of impact injury. The engineering design process is used to shape the entire projectile. The total weight of the projectile and its weight dispersion is essential to the projectile stability and the energy efficiency it offers. We polished the tips of the samples and measured their weight in Figure S4. We collected the samples prepared in the corresponding Figure 2. They will undergo dynamic tests, single or installed as a complete nonlethal projectile.

Six distinct sample formulations of polyurethane foams were used to test the air launcher and solid wall. From each formulation, we prepared three formulations to ensure potency during the experiments. Laboratory-made polyurethane foam samples are cylindrical with a convex head. We are highlighting the effect of the contrast in the processing direction on dynamic tests of mechanical behavior. Nonlethal projectile heads manufactured from various optimized formulas are shown in Figure 2a. Different nonlethal projectiles depend on the models available on the market.

To choose a suitable holder for nonlethal projectiles, we studied a group of materials with varying shock absorption capacities as follows:

Natural beechwood is a natural wood of medium hardness and softness, which has broad leaves and deciduous leaves and produces seeds, and its growth is prolonged, making soft hardwood. We chose the beech tree, a type of impact-resistant wood characterized by its lightweight and low cost.[42] We took six cylindrical samples 20 × 20 cm from different pieces of this wood, using an automatic cutting machine with high accuracy (Figure S5). Figure 2b shows the samples selected before and after automatic slicing.

Artificial plywood is manufactured by gluing thin sheets of pine veneer (density from 460 to 520 kg/m3). They are close to each other and distinguished by the fact that they resist expansion and shrinkage, are easy to form, and have multiple colors. It is dense and resistant to shock; combines lightness in weight, durability, and softness of touch; is distinguished from natural wood by its lack of influence from biological factors and resistance;[43] and is good at providing rigidity to structures. We took six samples from the artificial plywood panels and relied on a micro-cutting machine to obtain samples with dimensions of 20 × 20 cm for dynamic tests. The corresponding photos in Figure 2c show samples made of artificial plywood.

For instance, engineering design 3D printing makes it feasible to fabricate a nonlethal polyurethane foam holder portion (Figure 2d). Many models of different sizes and shapes can be predicted and produced into a 3D digital model to manufacture a nonlethal shockproof projectile mount. Also, manufacturing presents an economical speedway to manufacture molds with the exact dimensions as those sold in the market. We rely on the substance polylactic acid (PLA) used in manufacturing these stands,[44] which we strive to be environmentally and human-friendly simultaneously, and 3D prototyping.[45]

An engineering design approach reduces risks and achieves the necessary engineering limitations.[46] To research mechanical systems, measurements of nonlethal projectile holders are required. Therefore, we used two licensed programs, engineering and construction packages. The first program is SolidWorks,[47] with which we designed the solid 3D geometric shapes of the nonlethal projectiles holder part are given in Table S3.

We are using a Dassault Systems engineering computer application. We address engineering challenges associated with optimizing, compiling, and verifying safety-critical integrated software. The objective is to provide efficient and dependable manufacturing.[48] We relied on the XM1006 projectile as a reference in our study. The second program is CATIA design,[49] with the help of the 3D experience platform, where we develop several products with all of the innovative stakeholders and clients on our platform. We designed and printed two prototypes of the projectile holder (Figure S8). We simulated a dynamic study during a collision, and we will try to compare it with reality during realistic tests of samples. Furthermore, we use powerful 3D dashboards that drive real-time business intelligence and simultaneous design. A comprehensive product development platform that integrates seamlessly with processes and tools is a quantum leap toward reaching a final product developed with the required features.

Samples were 3D-printed from acrylonitrile butadiene styrene (ABS),[50] filament for fused deposition modeling (FDM).[51] The 3D-printed specimens were tested dynamically. The structure of these samples was analyzed in the same way as PLA. These ABS compounds with mechanical properties can be better than many other materials, such as wood, and are promising for their ability to combine with nanomaterials used in FDM 3D printing. Figure 2e shows samples of nonlethal projectile holders made of acrylonitrile butadiene styrene (ABS).

A variety of alumina (Al_2O_3) percentages was incorporated into high-density polyethylene (HDPE) to investigate the additive material effect on the consistency of high-density polyethylene projectile holders. The final product with the desired properties for the nonlethal application was controlled via mechanical analysis. Our research focuses on nanocomposites with a semicrystalline HDPE matrix strengthened.[52] This work is based on the characterization of mixtures

https://doi.org/10.1021/acsomega.2c06265
ACS Omega 2022, 7, 47129−47147

of HDPE/Alumina, the most commonly used thermoplastic polymer and hence an essential component in industrial plastics.[53] In the presence of a compatibilizer, mixtures of variable compositions of (2%−2.5%) by weight were prepared.

We were involved in analyzing HDPE/Alumina mixtures so that the optimum alumina ratio could be reached. We prepared the sample mixtures by the molding method in the molten state. The proportions of varieties used are 98/2, 97.5/2.5, and 97/3%. The samples of HDPE compounds are given in Table 3. For all compositions, structural and mechanical characteristics were carried out. Adding alumina to polymers improves mechanical properties. In this part, we have only manufactured the nonlethal projectile holder.

Table 3. Essential Compounds in the Preparation of HDPE

mixture	C.04	C.05	C.06
alumina (% by weight)	2	2.5	3

After an in-depth study of HDPE, we chose formulations with shock-resistant properties. Next, we made a nonlethal projectile holder using the molten pressure method with a steel mole of iron design. Finally, we painted a white balloon to give it a bright appearance after cooling the samples. Figure 2f shows what the pieces looked like after preparation.

2.4. Collecting Nonlethal Projectiles. We used foam lock spray adhesive NG1633 to stick the low-density polyurethane foam to the high-density stand. Here we are using foam adhesive spray to attach two sections of polymer. For a permanent bond, we sprayed both surfaces well. They are done by holding the foam 30 cm from the surface to be spread well and moving it to achieve a layer of adhesive until coated. Next, we let the adhesive dry until it feels sticky. This medium is the same method we use for the foam holder. Then we carefully align the foam to the holder because the glue often sticks so tightly that it is difficult to reposition once the two surfaces come into contact. Leave them for treatment for one hour only. We can see torn foam sections on the opposite wall surfaces when testing the bonding strength between the two polymer parts. They are evidence that the bond strength between the two molecules is stronger than the polyurethane foam.

We used six formulated test pieces to test the air launcher and the solid wall. The laboratory-made polyurethane foam samples are cylindrical with a spherical convex head attached to a holder made of HDPE. They are also done to highlight the effect of the contrast in processing direction on the dynamic tests of mechanical behavior. Nonlethal projectiles are manufactured from various optimized formulas, as seen in Figure 3a. The reference sample for nonlethal ammunitions XM1006 (Ep_R) is given in Figure 3b. Various nonlethal projectiles were designed based on models on the market.

Many researchers have focused on kinetic energy nonlethal (KENLW).[54,55] Various nonlethal projectiles have been manufactured based on existing models on the market. Fabricate nonlethal projectile models of the different optimal formulations of polyurethane foams. There are numerous stable forms, from solid to elastic projectiles.[56] The effects of such bullets are sadly unknown since it is impossible to quantify the energy passed on to the human body or the resulting deformation. We should therefore quantify and track the power to avoid actual harm. As seen in Table 4 describes the various models of projectile materials. Six polyurethane foam projectiles were used and compared to reference projectile XM1006. However, these projectiles should be characterized using a pneumatic launcher and a rigid wall.

The XM1006 has a high impact velocity of 80−105 m/s, much faster than the 70 m/s for the L5 and 90 m/s for the FN303. We've concluded that our nonlethal projectiles hit an impact velocity of 25−130 m/s, controlled by the pneumatic launcher and the preparation conditions. Developing nonlethal projectiles is more effective when predicting adequate information about operational engagement distances. The current work focuses on the issue of safety, i.e., the minimum requirements when using nonlethal missiles to avoid serious injury. Additionally, the maximum engagement distance may be calculated using existing data on the usage of nonlethal projectiles.

There are many producers of nonlethal munitions. However, few factories supply nonlethal ammunition to law enforcement

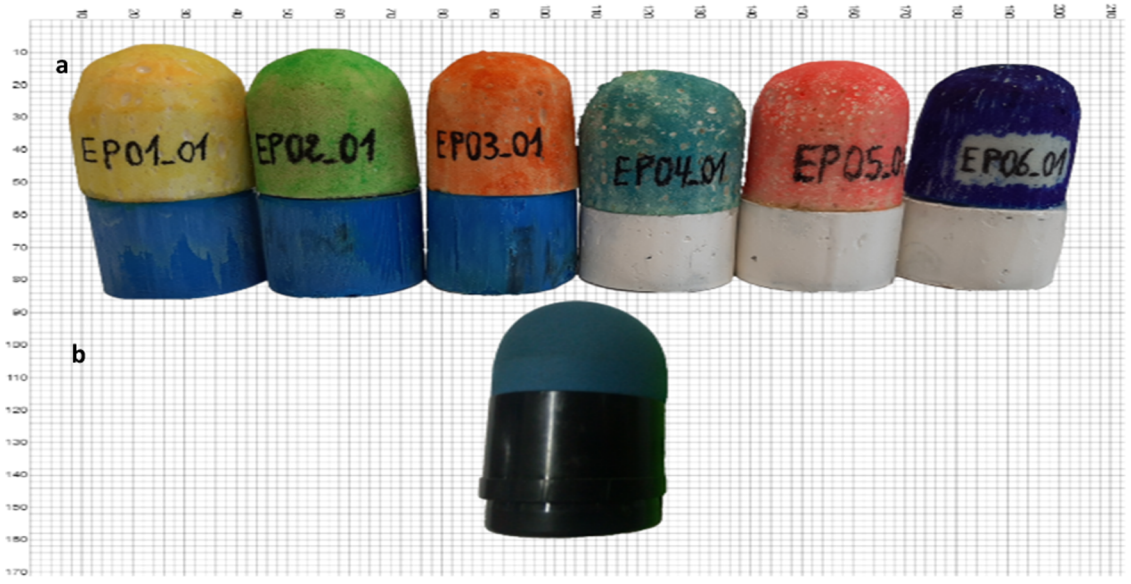

Figure 3. a. Range of specimens elaborated on nonlethal projectile polyurethane foam. b. Specimen referenced XM1006 nonlethal projectile.

https://doi.org/10.1021/acsomega.2c06265
ACS Omega 2022, 7, 47129−47147

Table 4. Material Model Nonlethal Antipersonnel Weapons[54,57,58]

Projectile	Manufactured non-lethal projectile models	XM1006	L5	FN303
Diameter [mm]	35	40	37	17.2
Mass [g]	23-29	26	30-140	8.5
Impact velocity [m/s]	25 - 130	80-105	70	90
Non-lethal projectile models				

personnel.[59] These manufacturers developed several guns, both 12 and 37/40 mm. The number and form of sub-munitions used and the defined velocity muzzle differ for these munitions. Table 5 displays the requirements for commercially produced nonlethal projectiles.

Table 5. Specifications for Commercially Produced Nonlethal Projectiles

ammunition caliber	submunition mass	velocity muzzle	products
37−40 mm	20−140 g	50−137 m/s	small bean bags and foam rubber projectiles[60]
7−20 mm	20−50 g	76−243 m/s	bean bags and rubber bullets[61,62]

The head is generally not targeted in government and military techniques, strategies, and procedures. However, specific unexpected incidents, such as a motion from the goal, can have a reluctant effect. Accidental head impact studies indicate that the nonlethal projectile will trigger meningeal harm requiring immediate treatment.[63] The thoracic effect evaluation is essential since several impacts may be predicted in this area.[60] The results of the experiments show that even at a range of 0 m, the criteria considered are ten times significant. Shots in the thorax are deemed exceptionally healthy in specific body areas. The accuracy checks often produce a good performance such that the launcher is consistent with precise strikes at a distance of 50 m.

The viscous parameter was well associated with the accident evaluation for studies on polyurethane foam. This criterion is only based on the features of the affected zone. SolidWorks was used for simulations. Figure S3 explains the manufacturing procedure for nonlethal projectile carriers and industrial model design.

If polyurethane foam is to play a structural role, the structure design must reflect the proper use of the foam. A high strength-to-weight ratio makes it easier for such structural applications when the externally applied force is low and well-distributed. Bending motions tend to disperse the pressure in a broader area, concentrating on interactions between vertical walls and roofs. In addition to the structural roles of foamed polyurethane in construction, it has two other necessary functional capabilities. Properly applied, it can provide outstanding thermal and acoustic insulation. It provides sound insulation mainly by rigidizing the nonlethal projectile panel components, thus decreasing their ability to retransmit vibrations.

In nonlethal projectile risk evaluation, many studies standardize the nonpenetrating effects of the chest and head, such as the STANREC 4744 study conducted by NATO.[64] Therefore, we will use the standard 40 mm nonlethal reference projectile to compare the results. In addition, we aim to study the current state of the art in SoTA requirements[65] and thresholds for assessing the risk of nonlethal kinetic energy impacts and their application to nonlethal projectiles.

2.5. Simulated Nonlethal Projectile Design. We evaluate the MEF of the XM1006 reference nonlethal projectile holder models that are straightforward to install and feature a circular inner bore. Thus, we used a finite element technique to study static pressure. We built a variety of grids to inspect the geometry of projectile holders to identify which grid type would yield the most significant results. We see that the effect begins to settle around 200 000 nodes. This has proven our choice of a tetrahedral network with a parametric surface and an intermediate smoothing-compatible procedure. As seen in Figure S7, circumferential drilling with a high-quality surface is rapid and precise.

Additionally, we found that forces and deformations transmitted linearly, indicating that the material generally had solid viscoelastic characteristics. The loads that determine the precise configuration and most forces also cause deformations in the nonlethal projectile holders. The maximum degree of leverage exists around the upper limits of the collision force's influence on the surface confronting the projectile impact. As a result, we see increased stresses,

Table 6. Experimental Simulated Study of Nonlethal Projectile Holders

substance	load (MPa)	deformation (10^{-3})	constraints (MPa)	displacement (mm)	mass (g)
PLA	0.3	4.65	18.33	0.20	28.6
	0.6	6.32	31.46	1.30	
	1	15.65	53.43	1.85	
ABS	0.3	6.90	22.60	0.98	25.5
	0.6	10.69	34.89	1.46	
	1	21.56	54.65	2.44	

https://doi.org/10.1021/acsomega.2c06265
ACS Omega 2022, 7, 47129−47147

displacements, and deformations when a structure is loaded. Comparing PLA to ABS, we observe that PLA outperforms ABS in fatigue, removal, and deformation, although ABS's nonlethal projectile carrier block is lighter in mass. The results are summarized in Table 6, and the qualities of PLA and ABS for use in nonlethal projectile holders are given in Table S2.

2.6. Characterization Dynamic. *2.6.1. Dynamic Mechanical Analysis (DMA).* Six polyurethane foam samples were subjected to the DMA test using Dynamic Mechanical Analyzers TA Instruments, a chamber for environmental testing, and a 5 kN dynamic load cell. Each foam type was sliced into the cylindrical sample in a loading parallel to the Alumina and MMT charge distribution. The samples measured 30 mm in diameter and 10 mm in height, as seen in Figure S6. Under uniaxial pressure, cylindrical pieces were placed perpendicular to the charge distribution direction, and 2% medium stress was applied to the samples. The strain oscillated in a sine wave pattern with a 0.3% amplitude and a 0.25 Hz frequency. The average strain and strain were chosen to preserve the stress within the linear stress/strain range for all six foam forms. The frequency enabled the DMA TA instruments to operate correctly to complete a sine wave stress cycle for all six composite foams. It was then heated at 01 °C/min from −80 to 200 °C to foam samples. Load and displacement information was analyzed, and all characteristics, including stress, storage modulus, strain, tangent delta, and loss modulus, were simultaneously calculated.

2.6.2. Pneumatic Launcher Tests. After preparing the foam samples, we examined the microstructure using an electron microscope. We select the open-cell formulation that does not contain microstructure defects. We also focus on distributing the filler on the cell walls rather than the lumpy filler between the foam cells. Six formulations were selected from the manufactured samples among many formulations, and each formulation was optimal. The weight of polyurethane foam varies according to its components and length-to-width ratio. The type and weight of the foam carrier also affect the shape and characteristics of the nonlethal projectile.

Six samples, each comprising three instances of the same composition, were evaluated. The test pieces were cylindrical, with a convex head from established formulas. The model is positioned into the pneumatic launcher, where static pneumatic pressure is applied. The length ratio ranges from 60 to 80 mm, and the diameter ranges from 35 to 35.6 mm. Also, the weight varies from 20 g to 29 g based on what each nonlethal projectile is made of. All data regarding test samples, as shown in Table 7.

The pneumatic launcher mechanism is smooth, and the breech is attached to a compressed air gas tank by manually controlling the projectile's speed. The speed may vary by changing the pressure. The pneumatic device enables home-made, nonlethal projectiles laboratory to be shot at different diameters. The impact of the projectile must be natural on the goal. The actual pressure depends on the gas bottle type and the compressor used. The overall pressure for this work was 10 bars maximum.

Table 7. Characteristics of the Used Nonlethal Projectile

projectile nonlethal	diameter (mm)	length (mm)	mass (g)
Ep_01	35.4	80	28
Ep_02	35.6	60	20
Ep_03	35.2	60	28
Ep_04	35.6	80	27
Ep_05	35.6	70	23
Ep_06	35.5	70	26
Ep_R	35	60	29

These experiments aim to evaluate nonlethal projectiles with a handmade pneumatic launcher. We calculate the energy density standard to determine the probability of skin penetration when firing at the human body. Hence, it must be remembered that the NATO protocol discusses firing to penetrate projectiles at a specified distance.[64] Therefore, various tests were carried out with the commercial XM1006 projectile, and we compared it to lab-made projectiles. Several tests have been conducted to assess projectiles based on the penetration depth of ballistic effects,[62] which depends on force−time, force−deflection, and deflection−time. In addition, gelatin may supply information on whether a particular product will lead to penetration into acute ballistic effects.[66] Finally, preliminary biomechanics verification presents the VC ongoing injury parameter assessment, which predicts the risk of projectile infection.

Several tests have been carried out on samples made of filled polyurethane foam. The nonlethal projectiles laboratory is designed and produced according to the XM1006 commercial projectile labeled as a reference projectile, which is named Ep_R, directly from the response of the missile on a rigid wall fitted with a sensor for piezoelectric force (see Figure S14). The scheme of the industrial mechanical production unit for the production of a rigid wall is shown in Figure S16. The projectile displacement signal of the rigid wall is created to track the velocity and force of the shell; the internal tracking system of the software oscilloscope allows for this to be accomplished. When two separate devices generate power and displacement signals, it must be confirmed that the signs are synchronized. This connection is regarded as the maximal impact force. Therefore, more than one experiment for each sample is achieved where the effects affect velocities. In all experiments, 5 bars of pressure are used. Figure 4 shows a pneumatic launcher made up of different parts that we designed and made to high standards. Figure S15 shows the method used to protect the components from rust and corrosion.

We ensure all components are present and practical before using the pneumatic launcher. We put the air tank used in the mouth of the operator. The cylindrical shape of the mouth helps adapt to various nonlethal projectiles. The air tank must always be tight enough to the muzzle for the operator's safety and to keep air from leaking. We hook up the DC 24 V power source to the control box, which powers the solenoid valves that control the operator. The black electric wire end must be connected to the ground of the voltage source. The red tip must be linked to 24 V. Then we open the compressor valve to allow the air to supply the pneumatic launcher.

We operate all of the measuring instruments, such as sensor amplification, speed sensor, piezoelectric force sensor, rigid wall antishock wall, power supply unit, etc. The projectile is loaded through the muzzle by pulling the moving part and placing the nonlethal projectile inside the barrel before closing everything tightly.

We adjust the necessary pressure via the control box with a digital display in the compressor. We can still use it by hand, but we can also set the pressure automatically. In automatic mode, the intake is turned on, and the solenoid valve

https://doi.org/10.1021/acsomega.2c06265
ACS Omega 2022, 7, 47129−47147

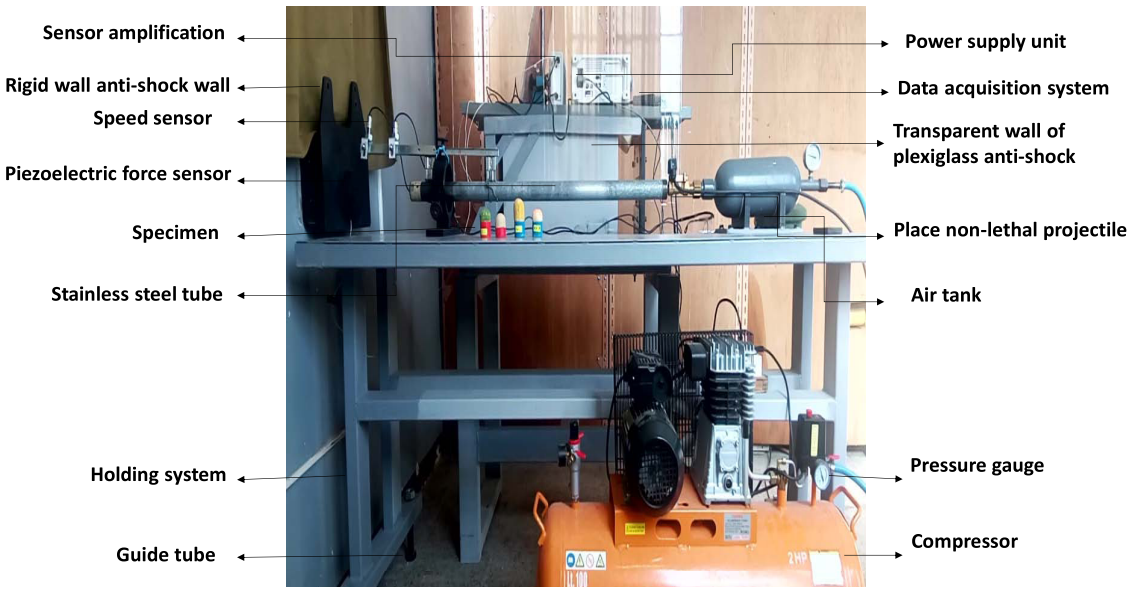

Figure 4. Overall sight of the pneumatic launcher.

automatically keeps the pressure around the predicted value. In this mode, the pressure tends to decrease over time. So, it is easier to control the launch pressure in a way that lets the launcher have a pressure gauge higher than what is needed and then let it drop on its own to the desired launch pressure. When we read the selected press on the cursor, we press the launch button.

2.7. Assessment of Injury Risk from Nonlethal Impacts. Propose nonlethal impact assessment methods for safe and effective use. There is a whole range of products on the market. But no prior research was done on the relationship between material qualities and harm levels induced by these projectiles. Indeed, different reported cases report severe injuries following this form of projectile. The XM1006 projectile impact projections are based on direct effects that can be stopped anywhere in the body with a projectile penetration that is often considered skin penetration. The authors would like to stress that, thanks to their comparatively small impact surface, their experience indicates that minimal (20 mm) nonlethal projects will exceed the maximum skin penetration more easily than primary projectiles.

We seek to advantage of the study conducted by kinetic energy nonlethal (KENLW) projectiles[55] for reduced lethality thresholds of concussion, coma, and damage. These projectiles are specially designed to impede people or stop them. Under normal circumstances of their use, they have a low probability of causing fatal outcomes or serious or permanent injury. This last one has severe symptoms on the human body, especially the brain and heart, the most critical and sensitive areas. In this study, these effects were explained physically. They allow us to measure the strength of projectile polyurethane impacts and compare them with their market counterparts to know the measurement effectiveness and avoid the deterioration of the human body. This study is rich in linking the structure of matter with its physical properties and biological effects. If the impact force of nonlethal projectiles is less than the damage threshold, in this case, we consider that the risk is negligible at this value, which is one of the norms. The possibility of injury is directly proportional to the transient intracranial pressure inside or to the maximum impact force on the human brain. There are several studies on brain injury thresholds DGA.[67]

Two criteria are used to predict the degree of brain damage caused by the nonlethal projectile's impact. The first criteria are continuous computerized monitoring of intracranial pressure (TICP),[68] and the maximum value at the threshold is measured throughout the post-mortem human subject (PMHS).[69,70] The second essential is the leading contact pressure force measured by an analytical model founded on the inside of the head pressure data. Table 8 summarizes the intensity of brain lesions as a function of the maximal TICP, as measured as a function of the contact pressure force.

Table 8. Measured TICP Values and Computed Maximum Contact Force Related to the PMHS Experimentation[36] [a]

injury severity	velocity (m/s)	maximum TICP (kPa)	maximum contact force (kN)
risk of loss of consciousness (<30 min)	35.7 ± 0.9	25	2.2
risk of cerebral hemorrhage and minimal risk of unconsciousness from fracture	42.9 ± 1	45	3.6
significant risk of fracture	56.7 ± 1.3	150	7.4

[a]Reprinted in part with permission from NATO Standard AEP-103 from ref 36. Copyright 2021, the NATO Standardization Office (NSO).

The TICP or contact strength thresholds, shown in Table 8, are data standardization results from effects on the head's temporal, parietal, or frontal region. The significance of transcranial pressure depends on the measurement point. According to the criteria values shown in Table 8, three standard speeds can be calculated. We compare the results with Table 5 and find that the two projectiles, FN303 and L5, have the highest impact velocities of 90 and 70 m/s, a value that exceeds the skull-breaking threshold of 56.7 m/s. The force-wall method says that the XM1006 can also break the skull when it hits 80−105 m/s. The manufactured nonlethal projectile models have an impact velocity range of 25−130 m/s. However, there can still be a risk of loss of consciousness

https://doi.org/10.1021/acsomega.2c06265
ACS Omega 2022, 7, 47129−47147

if the impact velocity is more significant than 35.7 m/s and a chance of cerebral hemorrhage if the impact velocity is greater than 42.9 m/s. However, it covers the safety range in the 25−35 m/s field, and we can also relate these impact velocities to firing distances based on the projectile delay. There are technical benefits to using the force-wall method to get a reasonable head impact estimate quickly. Table 8 gives a value of 7.4 kN, which seems to match the possibility of a fracture in the temporal part of the head.

2.8. Microstructural Characterization. *2.8.1. Scanning Electron Microscope (SEM).* The fabricated foam's microstructure was examined by electron microscopy, by Philips-type JEOL JSM 5800 functioning at 10 kV was put to use. A 1 mm breadth was cut off the foam samples in the x-direction. The pore measurement of the foams was identified from the images obtained from electron microscopy through the open-source ImageJ software. We have obtained good pictures that show how the loads are spread out on the surfaces of the polyurethane foam cells. ImageJ software evaluated the morphological characteristics of the polyurethane foam.

3. RESULTS AND DISCUSSION

3.1. Physical−Chemical Properties. As seen in Table 9, compared to PUR_1, the addition of alumina and MMT fillers led to an increase in viscosity. They might result from hydrogen bonding and Van der Waal forces between groups active in the filler particles and the polyol.[71] Due to alumina (Al_2O_3), the rise in viscosity was from 430 to 1100 mPa × s and 1650 mPa × s, respectively. Including the montmorillonite (MMT) addition, the viscosity rises from 650 to 1340 and 1980 mPa×s, respectively. All PUR mixes exhibit non-Newtonian behavior and is analogous to PUR mixtures, including various types of mineral fillers.

Table 9. PUR Systems' Dynamic Viscosity η [mPa × s]

foams	10 rpm	20 rpm	30 rpm	100 rpm
PUR_01	430 ± 9	320 ± 10	245 ± 8	120 ± 8
PUR_02	1100 ± 10	620 ± 11	420 ± 9	210 ± 7
PUR_03	1650 ± 12	1350 ± 12	650 ± 10	330 ± 7
PUR_04	650 ± 10	480 ± 8	365 ± 9	150 ± 6
PUR_05	1340 ± 11	760 ± 10	520 ± 10	240 ± 8
PUR_06	1980 ± 10	1435 ± 11	760 ± 9	310 ± 9

3.2. Characterization Dynamic. *3.2.1. Dynamic Mechanical Analysis (DMA).* The peak tan δ is the ratio of loss modulus to storage modulus, a measure of the damping capacity of the material. In contrast, the peak G' is the storage modulus, representing the elastically stored energy. Also, G'' is the loss modulus, meaning the energy absorbed plus dispersed as heat. The loss factor represents the ratio of dissipated energy to elastically stored energy. The loss factor is widely used to quantify energy-absorbing capabilities.

Figures 5 and S2 show the viscoelastic properties of PUR samples of varying densities using DMA TA instruments. The data vs. temperature plots were created to establish the foams' temperature sensitivity. In that order, the PUR 01 and PUR 03 plots revealed different transition zones and a tangential delta peak at about 129.48 and 121.41 °C. This peak corresponds to the material's glass-transition temperature (T_g). During this transition, the material becomes ductile, and the loss modulus and storage fall proportionately.

The viscoelastic behavior was comparable for PUR 01 and PUR 03 but different for PUR 02, changing slowly over the whole range of temperatures, with a tangential delta peak at 119.17 °C. This distinction between the alumina-containing samples indicates that a certain percentage of filler changes the viscoelastic behavior. The behavior of polyurethane foam under compressive force is subject to the deformation of the unit cell wall structure. They are attributed to the fact that increasing the bending and torsional stiffness of the unit cell wall structure through alumina increases mechanical properties like structural rigidity, energy absorption, and strength under compressive load.

Similar patterns and behaviors were seen in viscoelastic materials. PUR_04 and PUR_05, and PUR_06, but different for PUR_01 and PUR_02, and PUR_03. With or without alumina, introducing montmorillonite affects the viscoelastic characteristics of MMT-reinforced PUR. When it comes to materials, the material's behavior under compressive load is determined by distorting the unit cell wall structure.[72]

The inclusion of reinforcing MMT can increase the mechanical characteristics of foams. They are due to the unit cell walls with enhanced stiffness in bending and buckling caused by the reinforced MMT that improves the mechanical

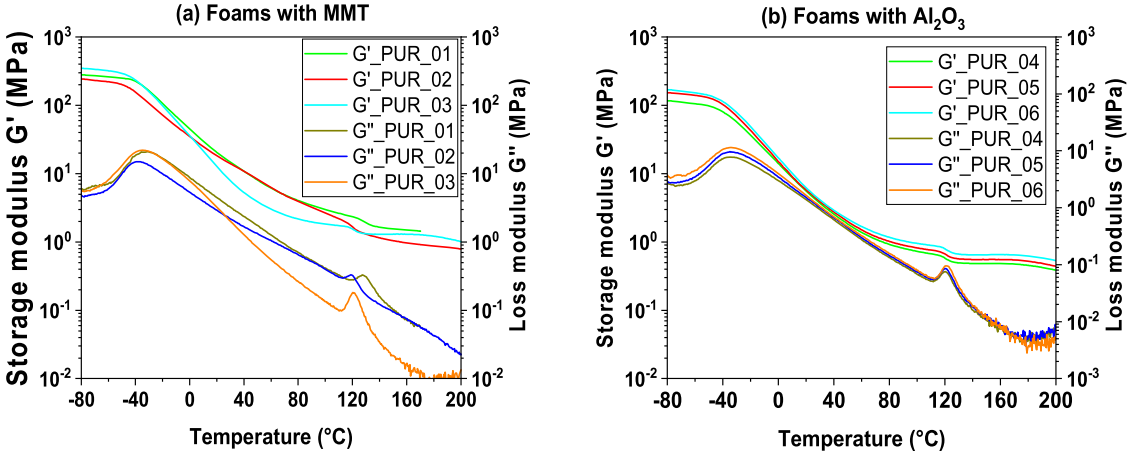

Figure 5. (a) DMA tests for reinforced polyurethane foam with Al_2O_3. (b) DMA tests for reinforced polyurethane foam with MMT. T = −80 at 200 °C, f = 1 Hz, ΔT = 3 °C.min^{-1}.

https://doi.org/10.1021/acsomega.2c06265
ACS Omega 2022, 7, 47129−47147

aspects of the structure, strength, stiffness, and the structure's energy absorption capability under compressive stress. Thus, it is critical to ensure that the MMT adds strength, energy dissipation, and stiffness. In addition, the foam functions as a matrix, resulting in a lightweight, low-density composite material that acts as an insulator in some applications.[73]

Compared the Figure 6 and Table 10, PUR 01 has superior viscoelastic characteristics at 130 °C. Compared to PUR 02

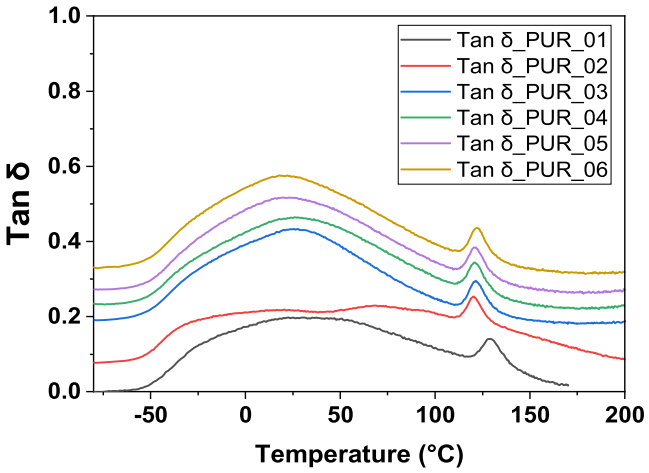

Figure 6. Tan δ curves: outcomes of DMA testing.

Table 10. Test Results of DMA

foams	$T\alpha$ °C	T_β °C	Tan δ max °C	Tan δ max
PUR_01	−31.82	129.48	129.48	0.162
PUR_02	−38.32	118.59	119.17	0.190
PUR_03	−34.46	121.46	121.41	0.121
PUR_04	−34.36	121.76	121.26	0.132
PUR_05	−34.34	121.01	121.01	0.130
PUR_06	−33.63	121.62	122.16	0.126

and PUR 03, it has weak viscoelastic attributes between 119 and 122 °C. It is owing to their loss moduli and high storage reflecting elasticity and viscosity, respectively, of the loaded polyurethane foam by alumina. Nevertheless, PUR 04 and PUR 05 exhibit less viscoelastic characteristics than PUR 06 at temperatures less than 122 °C. Due to the elasticity and viscosity of loaded polyurethane foams by MMT. The load type, proportion, and distribution in the polyurethane foam matrix are controlled by the dynamic properties of the foam at a significant temperature. We conclude that the prepared polyurethane foam showed considerable flexibility and viscosity in a strict middle. We can restore polyurethane foam to its natural state with several uses with a pneumatic launcher. It is a significant outcome, given that the PUR examined in this study was shock-resistant at high temperatures.

3.2.2. Pneumatic Launcher. Based on dynamic testing to analyze foam-filled impact behavior. The nonlethal projectile parts obtained from strength curves in terms of time are summarized. Table S1 summarizes the most important values that highlight the ability of these samples during the collision. We see that the power and length of the pulse increase as the piece's solidity and density increase. There is a connection between the microstructures of the projectile cortex and the actual effect.

Table S1 concludes that polymers are the most effective shock absorption. Despite the shock strength, the tested polymers remained resilient, unlike the cracked wood, considered dangerous. By applying a pressure of more than 10 bars, we notice that the speed increases with the increased pressure, leading to a significant force. The results demonstrate that HDPE is the best material for a nonlethal projectile holder.

The dynamic tests were carried out on nonlethal projectiles, which we installed well, i.e., the projectile head made of polyurethane foam stuck to its holder of high-density polyethylene. We performed in a room isolated from the personnel. The results showed similar behavior to the projectiles made and those sold on the market, such as the reference projectile XM1006. Figure 7 shows the dynamic curves obtained after filtering with Matlab.

The result will be displayed as an electrical pulse proportional to the force generated during the impact. The piezoelectric sensor has a sensitivity of 56.2 mv per 1 KN. There is a requirement for processing the oscilloscope's output with MATLAB software to obtain the force's natural evolution curves as a time function. Signals recorded by impact force sensors require further synchronization. The Supporting Information describes the sensor characteristics and filters used in Figures S9−S13.

We note from the curves that the development of the force during the impact is in the form of a peak and that the maximum value of the force is proportional to the starting energy potential; this was caused by the impact's great kinetic energy, which generates a large impact force compared to low energies. We also note that the strength signals do not reach zero and the presence of small peak curves is because the material needs time for the total recovery of the structure during the shock. In addition, the polyurethane foam structure has an elastic viscosity that distinguishes it from other materials.[74]

The findings suggest a strong balance between the graphs of the manufactured projectiles and the curves of the XM1006 reference projectile, especially the sample (EP_02), in calculating the peak impact force on the head for side effects. Measurement results with XM1006 missiles are significant for developing evaluation methodologies.[66] In addition, there is complete consensus on the nonlethal effects.[75] The maximum impact of head force can be suggested as a criterion for injury.

Since we conducted three tests for every three samples of the exact composition of polyurethane foam to ensure the homogeneity of the material and study its dynamic response under the same experimental conditions, we noticed that all of the curves are almost identical. In the case of the experiment on EP-03 projectiles, we note that the curve Ep03_Test01 has a slight displacement, which can be due to the presence of air vesicles inside the polyurethane foam formed during mixing, which led to a decrease in shock absorption.

This study is comparable to experimental test curves for industrial and commercial projectiles. Nevertheless, the experiment's shock sensor provides accurate readings anytime the air pressure causes a significant impact. The pneumatic launcher trials saw lesser deformation, cracking, and densification. They note that the identical features and dimensions stimulated all samples before and after the test.

Tests are carried out on foam samples of standard density and the thickness required. The stress curve produced by the findings may not be adequate since the laboratory shock meter

https://doi.org/10.1021/acsomega.2c06265
ACS Omega 2022, 7, 47129−47147

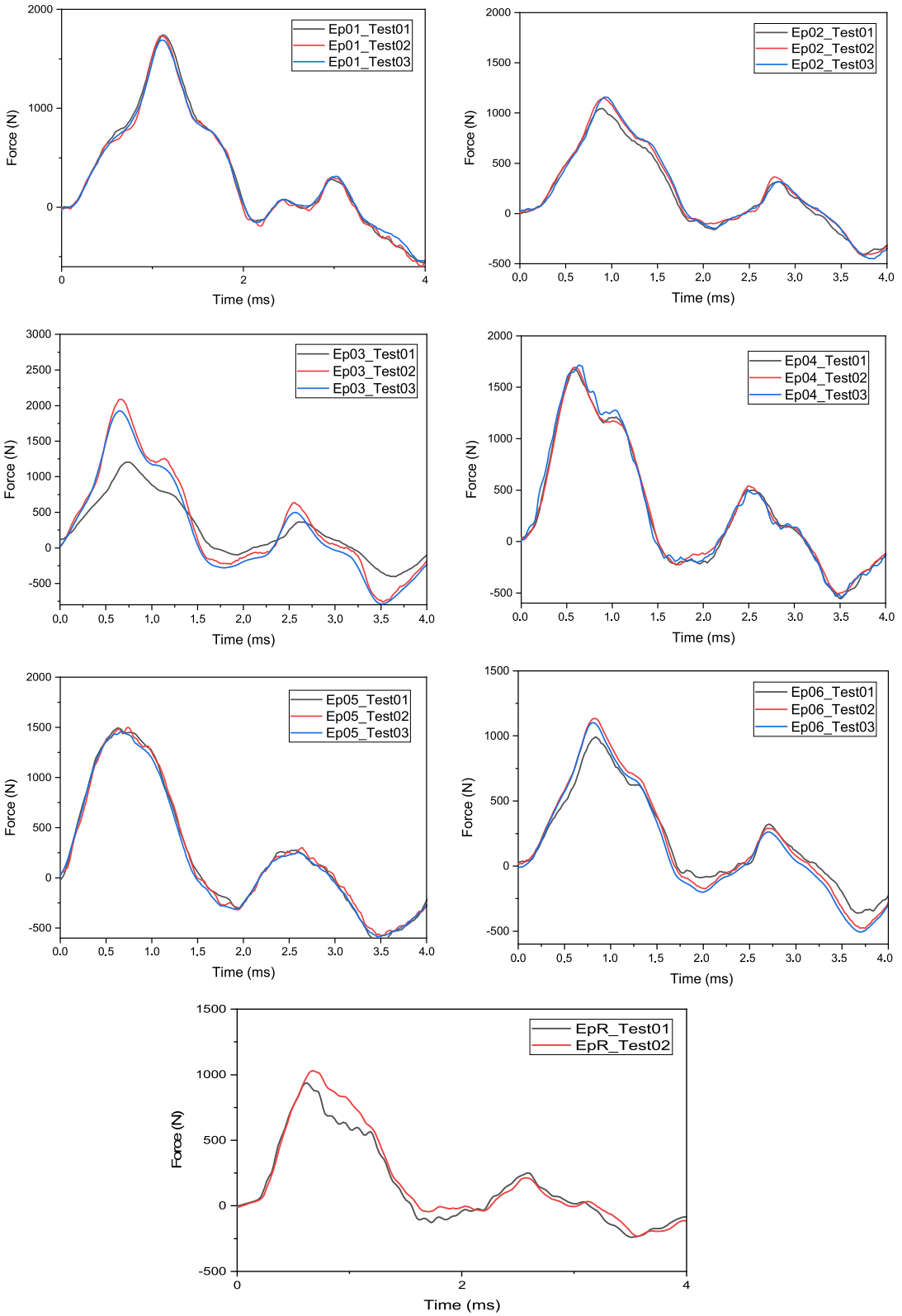

Figure 7. Properties force−time of the nonlethal projectile with pneumatic launcher.

is undergoing testing and cannot measure the condensation component of foam pressure. Therefore, if necessary, it is possible to extrapolate the curve partially. Thus, before any foam material can be employed confidently in nonlethal projectile impact operations, it must be identified by component-level physical testing. Then, reasonable confidence can be developed in predicting the injury parameters indicated.

The mechanical characteristics of the foam would depend to a large extent on the microstructure and the raw material of the foam cell.[76] Scanning electron microscopy (SEM) and 3D CAD models were used to examine the link between the

https://doi.org/10.1021/acsomega.2c06265
ACS Omega 2022, 7, 47129−47147

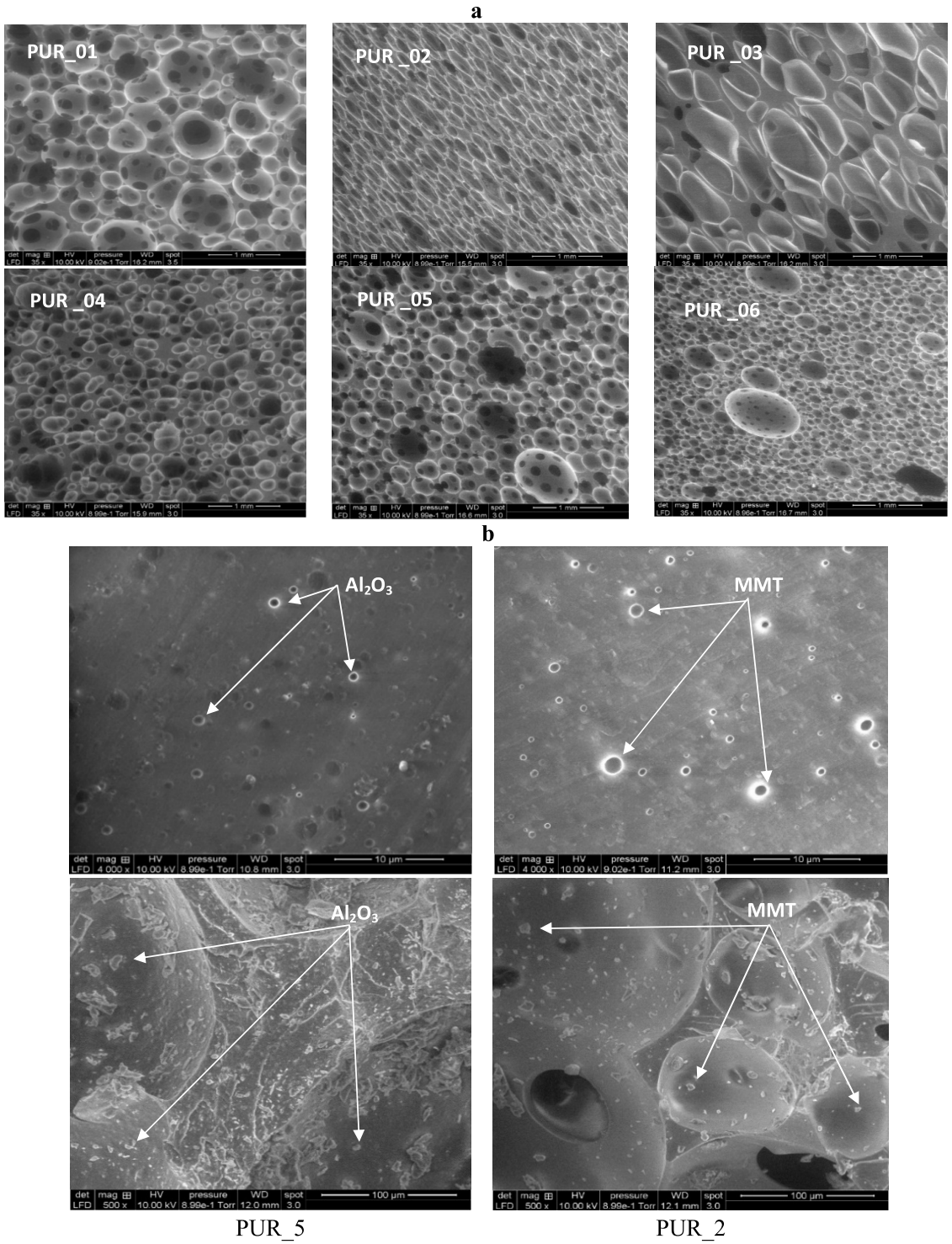

Figure 8. (a) SEM images showing the shape and distribution of the pores of the prepared polyurethane foam. (b) SEM images showing the shape and distribution of Al_2O_3 and MMT mineral fillers on polyurethane foam cell walls in a 10 and 100 μm unit.

macroscopic mechanical characteristics of the foam's microstructure. The pneumatic launcher tests were in good accord with the experimental results of polyurethane foam. The provided method will be instrumental in investigating the influence of engineering features of PUR foam on the macroscopic mechanical characteristics and indicative fabrication methods for antishock applications. Understanding the link between microscopic geometric features and visible mechanical parts is critical for developing the high mechanical qualities of foam products.

3.3. Microstructural Characterization. *3.3.1. Scanning Electron Microscopy (SEM).* We show SEM images in Figure 8a,b. The foam pore shows a spherical geometry. More pressure causes more deformation because the diameter of the individual foam holes decreases. The gaps in the walls of the cells, which indicate the presence of overlapping foam pores,

https://doi.org/10.1021/acsomega.2c06265
ACS Omega 2022, 7, 47129−47147

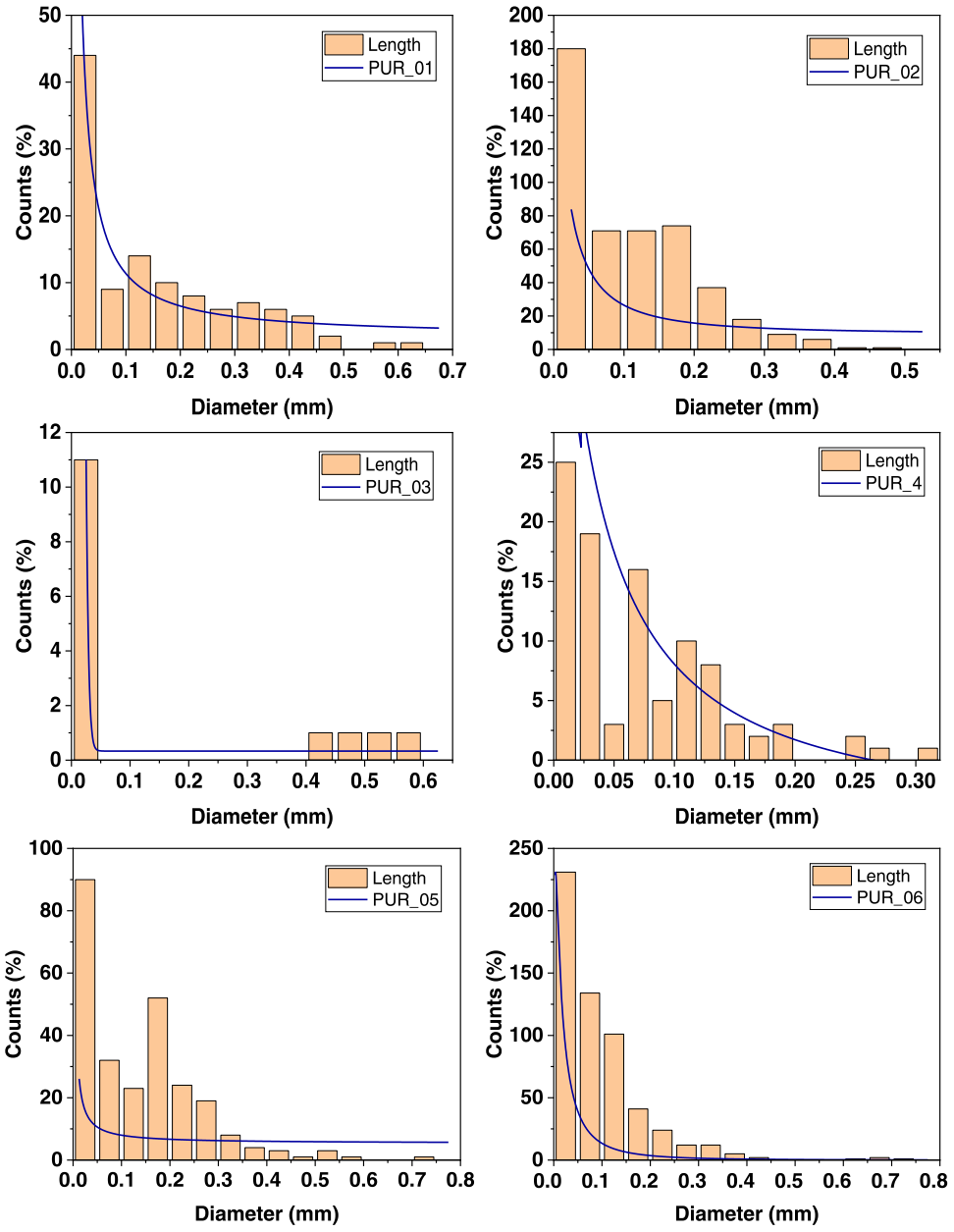

Figure 9. Histogram depicting the distribution of the mean pore width of the many PUR materials manufactured.

can be seen in the images of the foam treated at different pressures.

The effect of pressure on the corresponding density of the polyurethane foam and the volume fraction of the open and closed foam cells measured after dynamic experiments is shown. The related foam density increases after the shock phase and decreases after several hours. The foam's pore size ratio also increases with the development of the treatment pressure. Foams under increased pressure of 5 bar reach a higher relative density than foams at smaller force. Generally, the period after dynamic tests affects the corresponding thickness of foams.

Polyurethane foam cells are primarily spherical and semi-open in the studied density range. MMT and Alumina particles are dispersed evenly throughout the polyurethane foam matrix, showing that the studied foams are characterized by an overlapping open text cell irrespective of the filler type. Image analysis was used to estimate the apparent density distribution of cells' size of a roll of polyurethane foams. The lower cell size appears most likely due to the effect of the filler kernel. Moreover, this effect can be enhanced by residual water on the surface of the particles, causing added carbon dioxide to be released.

Figure 8b shows this crucial characteristic by enlarging a typical polyurethane backing to 10 μm and 100 μm overstatements. The higher-magnification image shows that the cell walls are fragile, only a few microns thick. As a result, the majority of polymerization occurs inside the supports. It is possible to generate smaller cells by increasing polyurethane foam density. The structure maintains its homogeneousness, and the cell diameter is constant. Cell walls are usually thicker at greater density. Cell walls are wrinkled to highlight the places of interaction between adjoining cells. These reaction regions consist of continuous thin polyurethane membranes that serve as cell barriers. A cellular scaffold is formed when several cells combine to create a foam.

https://doi.org/10.1021/acsomega.2c06265
ACS Omega 2022, 7, 47129−47147

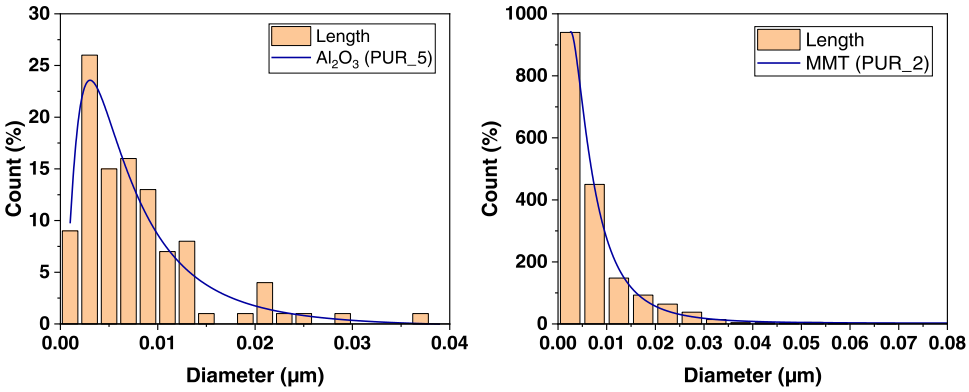

Figure 10. Histogram of the particle size distribution results of the various mineral fillers.

Figure 9 shows the average pore diameter distribution graph for various manufactured polyurethane foams. The foam cells' void content is comprehensive compared to the filler used. We note the distribution of cells in the form of a bubble. The cell wall is covered with a nano-alumina (Al_2O_3) and montmorillonite (MMT) filling, where the coverage of these fillings is more significant than the area of the foam's pores. The effect is that the filler qualities determine the characteristics of the foam. Its properties are particle morphology, crystal structure, and size.

We noticed that the mean pore widths were distributed more evenly in the PUR_01 and PUR_02 matrices from 0 to 0.5 mm. In the case of the mean pore width of the cells in the PUR_03 matrix, they were empty from 0 to 0.4 mm. The majority of the pore width was 0.4 to 0.6 mm. This distribution of the width of the mean pore of the polyurethane foam cells was due to the MMT filler. It is also responsible for the mechanical strength of polyurethane foam. Compared with the results of the pneumatic launcher for Ep03_Test01 projectile by PUR_03 foam. That explains why adding a percentage is superior to 9 wt % on MMT and leads to the appearance of defects in stress concentration. They are quickly causing holes in the structure of the polyurethane foam that has been made, which hurts the foam's mechanical performance.

In addition, the mean pore widths in the PUR_04 matrix ranged from 0 to 0.3 mm, and the mean pore widths in the PUR_05 and PUR_06 matrix ranged from 0 to 0.7 mm, respectively, and they were homogeneous. The mean pore width distribution shows that alumina can significantly provide distribution through the polyurethane matrix.

The particle size distribution of mineral fillers was determined in a manufactured PUR matrix dispersion. Figure 10 illustrates the distribution of particle sizes of the montmorillonite MMT and alumina. The results suggest that the particle size of MMT is 0.04 μm and alumina is 0.09 μm in all positions. The maximum proportion of particles for mineral fillers is seen at 0.01 μm. There was no accumulation of alumina and montmorillonite particles. Their concentration grew to a nanoparticle ratio of 0.01 m. As a result, they have a considerable surface area compared to size, widely scattered giant cell windows of polyurethane foam. At this concentration level, the fillers produce a dense network of micro-cells that interact with various soft segments on a dense network of polymeric cell windows. In addition, it significantly increases the hardness, with alumina containing 6 wt % and montmorillonite containing 6 wt %.

Because the polyurethane supports are constrained by open foam cells, MMT and alumina powder particles are counted as given in Figure 10. As demonstrated, raising the fillers percentage resulted in a slightly higher particle density within the cell walls and supports. Additionally, some metal powder separates from the polyurethane after fracture, leading to small dimples.

3.3.2. Descriptive Statistics. The cells were spread out in the polyurethane foam matrix with different average diameters of 0.070−0.142 mm. In contrast, the alumina filler had an average diameter of 8 nm, while the MMT filler had an average diameter of 7 nm. Alumina nano-reinforced polyurethane foams have more cells and a more robust matrix structure than MMT-reinforced foams. This makes them more thermally and mechanically stable and improves the cytoskeleton. Table 11 describes the dispersion of polyurethane foam cells and filler.

Table 11. Radius Characteristics of Polyurethane Foam Cells and Filler Material

foams	dimensions	maximum	minimum	mean (average)
PUR_01	diameter (mm)	0.643	0.004	0.15
	area (mm^2)	0.325	0.0000174	0.036
PUR_02	diameter (mm)	0.497	0.004	0.104
	area (mm^2)	0.194	0.0000174	0.015
PUR_03	diameter (mm)	0.577	0.004	0.142
	area (mm^2)	0.262	0.0000172	0.052
PUR_04	diameter (mm)	0.304	0.004	0.072
	area (mm^2)	0.073	0.0000174	0.007
PUR_05	diameter (mm)	0.718	0.004	0.135
	area (mm^2)	0.406	0.0000171	0.026
PUR_06	diameter (mm)	0.741	0.004	0.089
	area (mm^2)	0.432	0.0000171	0.013
MMT	diameter (μm)	0.090	0.001	0.007
	area (μm^2)	6.080	0.001	0.09
alumina	diameter (μm)	0.040	0.001	0.008
	area (μm^2)	1.130	0.001	0.08

Alumina and MMT may enhance the adherence of filler particles to the intervals in the polymeric matrix, resulting in the cellular morphology of PUR composites becoming more stable. The PUR structure is cross-linked and includes filler particles that might act as a barrier to cell adhesion, do not collapse during expansion, and generate extra edges capable of capturing CO_2 released by the cells.[77] According to Abdollahi Baghban et al.,[78] the enlargement of the pore size is related to the hydrophobicity of the filler surface; hydrophobic fillers

https://doi.org/10.1021/acsomega.2c06265
ACS Omega 2022, 7, 47129−47147

have a more vital adherence to the matrix of polymers, whereas hydrophilic fillers have a lower adhesion and a foam structure with larger cell size. This trend was also observed in our study. PUR_3 has the most considerable cell width among the PUR foams studied, owing to the extremely hydrophilic characteristics of MMT. Acetic acid treatments improve the hydrophobicity of MMT, resulting in more homogeneous cells with smaller diameters in the resulting PUR composites.

3.4. Assessment of Injury Risk from Nonlethal Impacts. The polyurethane foam projectile is secure, except at a limited distance. With a pneumatic launcher, all of the effects yielded good results. Therefore, the only available standard for estimating the probability of accidents appears reasonably practical and can be seen in actual implementations. The performance of the projectile is a more complicated issue. However, it is necessary to control the aspirations of the users. Although protection and efficacy genuinely support the findings, doctors should be mindful of potential unique lesion aspects of impact bullets, contributing to injury in the absence of penetration. As with most forms of severe blunt trauma, ultrasound and densitometry can probably be regularly conducted by doctors since any chest, or upper abdominal fractures can be deemed life-threatening. This paper is ultimately the first step in the required direction in which the community can better understand the efficacy and mechanisms of nonlethal projectiles.

To better comprehend these results and better analyze the problem of efficacy, an outcome is typically not always correlated with pain. Eventually, effectiveness can be described as compliance to protect it or other citizens (civilians or police officers).

They should be borne in mind compared with other potential focus categories, such as cases of war or crowding and rioting management scenarios, where the characteristics of individuals could vary considerably. More generally, utilizing nonlethal polyurethane projectiles as an intermediate enables the force to scale up or de-escalate slowly and understand how essential or aggressive the target's activity would be by watching the target's response. Some conclusions can be drawn. Using nonlethal bullets, in general, and polyurethane foam, in particular, eliminates aggression when nonlethal arms or other means have been likely to have a more detrimental impact.

3.5. Discussion. To achieve good results, we must respect the firing rules for nonlethal projectiles, the most important of which is the target area. In Figure 11, we summarize the permissible contingencies and the prohibited regions using nonlethal projectiles.

Designers will use nonlethal projectiles within the suspect's intended target area according to the overall conditions at the deployment site, established safety priority, and the force that is reasonably necessary to establish or retain situational control. As shown in Figure 11, correct areas (a) are the most appropriate primary target areas with the most muscle tissue and the least quantity of vitals, including the forearm muscles (zone 1), the thighs, buttocks (zone 2), and legs (zone 3). When the menace is manageable and the location is feasible, it is necessary to consider it first due to its low probability of injury. The abdomen and groin areas are the secondary target areas with a higher potential for injuries when hit by nonlethal projectiles due to the absence of muscular density. Intentionally target the abdomen area if the area (a) is inaccessible due to confrontation dynamics, prior influences

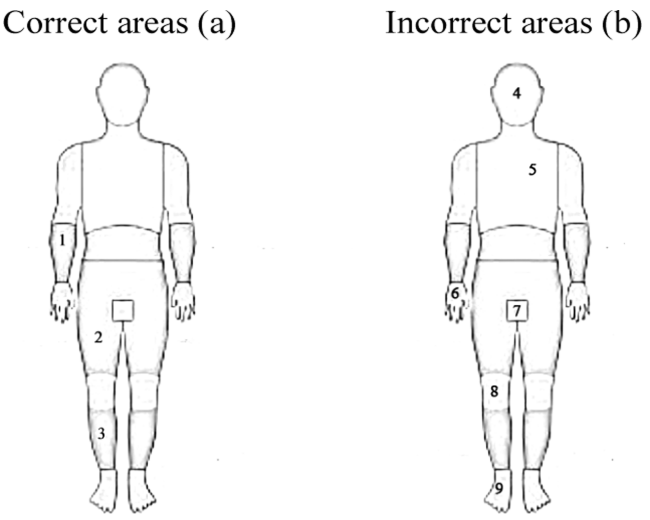

Figure 11. (a) Correct areas for nonlethal projectile targets. (b) Incorrect areas for nonlethal projectile targets.

are ineffectual, or the police authority has reasonable grounds to suspect that the subject will not be influenced by the impact on area (a).

Incorrect areas (b), which include the spine, and head (zone 4), the central mass of the chest (zone 5), and the genital area (zone 7), is the lethal danger areas with the most significant potential severe bodily harm or even death of the subject. In addition, there are sensitive areas due to a lack of muscle tissue, such as the hands (zone 6), knees (zone 8), and bottom of the feet (zone 9). Therefore, targeting in this area should be avoided except when the officer using nonlethal projectiles reasonably believes that the issue presents an impending lethal danger and that the deadly cover authorities cannot engage the subject or prevent them from doing so.

Potential secondary target areas such as the shoulder joint and arms are deficient in muscle density because the systema skeletale predominantly constructs these regions. Due to muscle tissue deficiency, the shoulder joint and arms must have a limited capacity to absorb kinetic energy from nonlethal projectiles and adequately distribute it to the body. Therefore, there might be instances in which the shoulder joint and arms are the most workable areas that present themselves as destination targets in a confrontation. Still, they must be considered carefully before shooting at them due to their movement. The neck and renal regions are possible targets in some instances where area (b) effects are ineffective.

This research aims to determine the effect of additives on polyurethane foam products, which form the basis of nonlethal projectiles. This new model will be multiapplication and stress-resistant. We evaluate the mechanical and morphological properties of the polyurethane foam after applying sufficient force with the manufactured pneumatic launcher. Mineral fillers significantly increase polyurethane foam's structural strength and shock absorption. In these cases, modification of the foam's dissipative characteristics is necessary to maintain safe internal stability. The present work arises from altering the properties of the shock transmission of the foam that makes up the head of nonlethal projectiles. Assume that this application will include the utilization of mineral filler-containing foams. In this scenario, it is necessary to examine the influence of the filling phase on the material's properties. We evaluated the strength of polyurethane foam. The interplay of viscoelastic

https://doi.org/10.1021/acsomega.2c06265
ACS Omega 2022, 7, 47129−47147

properties of polyurethane foams with various mineral filler ratios may have been replicated throughout the densities tested. PUR foam is produced using fumigants to form voids in the polyurethane foam mold. A suitable amount of DCM is employed to obtain a highly low density. In addition, polyols and isocyanates are mixed to generate liquid carbon dioxide, which may absorb heat and transform it into carbon dioxide gas.

In counter-terrorism and antiriot operations, it is essential to predict the impact of ballistics to assess safety. Multiple computed tomography-based head finite element models must be developed, or magnetic resonance (MRI) scans must be acquired to accommodate genuine head morphologic variation in dynamic head injury reactions.[79] In this study, the focus is on using SolidWorks software to simulate the ejaculation process. Some have used the LS-DYNA software for the same purpose, using the AM50 hypothetical human percentile model to predict skull fractures.[80] The FE models investigated dynamic head responses between people with varying head shapes.[81]

Polyurethane foams are distributed fillers incorporated into a bubble distribution in microstructure investigations. Also, successfully replacing hazardous ingredients in nonlethal weapon manufacturing can minimize costs and environmental effects. In addition, polyurethane foam production may help reduce road accidents and increase the polymer industry's sustainability.[82]

4. CONCLUSIONS

Six nonlethal projectiles were made. We built convex heads from polyurethane foam, adding alumina and MMT fillers increased viscosity. We chose a nonlethal projectile holder using the dimensions of commercially accessible designs to reduce the impact force. We utilized CAD modeling in SolidWorks to model nonlethal projectile deformation. 3D-printed polymeric nonlethal projectile holders have been developed, which is crucial to generating high-performance products.

We performed and evaluated a DMA. A tangential delta peak at 129.48 and 121.41 °C was seen in the PUR 01. In addition, PUR 03 plots the properties of DMA, about 129.48 and 121.41 °C. This peak represents the glass-transition temperature (T_g). During this transition, the material's loss modulus and storage decrease. Unlike the other samples, PUR 02 exhibits a gradual change over the whole temperature range, with a tangential delta peak at 119.17 °C. Due to their high loss moduli and high storage reflecting the polyurethane foam's particular elasticity and viscosity, respectively., PUR 01 and PUR 02 have better viscoelastic properties between 118 and 130 °C. Then PUR 3, PUR 04, and PUR 05 have superior viscoelastic properties to PUR 06 at temperatures below 122 °C and above 123 °C. They are relevant since the PUR in this research was tested for high-temperature and shock resistance.

We designed and manufactured a multicomponent pneumatic launcher and a rigid wall constructed in many stages to strict specifications. This pneumatic launcher evaluated the impact of nonlethal projectiles and the impact speed.

Based on dynamic testing to analyze polyurethane foam impact behavior. We see that the power and length of the pulse increase as the piece's solidity and density increase. There is a connection between the microstructures of the projectile head and the actual effect. Dynamic tests were done on nonlethal projectiles, and the results showed that they behaved the same way as XM1006. The produced projectile graphs and the XM1006 reference projectile curves, notably the sample (EP 02), show a solid balance to forecast the maximal impact force on the head for side effects. Therefore, the XM1006 measurement findings are essential for creating assessment strategies.

The technique of pneumatic launcher testing will help determine how engineering elements of PUR foam affect macroscopic mechanical properties and production procedures for antishock applications. Understanding the relationship between tiny geometric parts and visible mechanical components is key to designing high-quality foam products. Polyurethane foams are the best shock absorbers. In addition, the findings show HDPE is the best nonlethal projectile-holding material.

For the operator's safety, it stops people from getting into the protective cage as long as the operator's pressure is still on it. We recommend always using an eye protector and an ear guard during imaging procedures. Even though there is a transparent wall of plexiglass antishock to protect you, you should always stand behind the firewall to avoid broken glass from the cage itself. It would also help if you ensured that the air launcher was not loaded before the tests began and that nothing in the firing path would get in the way of the target. You also shouldn't use projectiles that aren't right for the pneumatic launcher or that could break or destroy themselves. This could cause the pneumatic launcher to get clogged or damaged, which could be dangerous for the user and the working environment.

SEM was used to look at the structure of the cells, the average size of the pores, and the size distributions of the mineral filler particles.

Foam cells are primarily spherical and semiopen in the investigated density range. The MMT and alumina particles are uniformly spread throughout the polyurethane foam matrix, indicating that the examined foams have overlapping open text cells. A photograph of a roll of polyurethane foam was taken to assess cell size dispersion.

We discussed nonlethal injury risks. We must respect the firing rules for nonlethal projectiles, the most important of which is the target area. Designers will use nonlethal projectiles in the suspect's intended target area based on site conditions, safety priorities, and the force needed to establish or keep situational control. When nonlethal weapons or other measures would have had a more damaging effect, the employment of nonlethal bullets in general and polyurethane foam in particular decreases aggressiveness.

■ ASSOCIATED CONTENT

Supporting Information

The Supporting Information is available free of charge at https://pubs.acs.org/doi/10.1021/acsomega.2c06265.

Polyurethane foams are manufactured after a free expansion process; dynamic mechanical analysis (DMA) results on polyurethane foam; nonlethal projectile holder construction process and custom industrial model design; technology for polishing nonlethal polyurethane foam tips; used sample cutting machine; method for measuring test samples; cutting of polyurethane foam samples by an automatic grinding machine; printing machine is used to make nonlethal ballistic carriers; piezoelectric force transducer used;

https://doi.org/10.1021/acsomega.2c06265
ACS Omega 2022, 7, 47129−47147

torque arm for sensor clamping; sensor acquisition card; SEFRAM oscilloscope; speed sensor; laboratory-made rigid wall parts; method used to protect parts made from rust and corrosion; industrial mechanical production unit scheme for producing a rigid wall; measurement data for dynamic characterization by air launcher of various parts of nonlethal projectiles; PLA and ABS characteristics for making nonlethal projectile holders; and deformation simulation SolidWorks of nonlethal projectiles (PDF)

AUTHOR INFORMATION

Corresponding Author

Noureddine Boumdouha − *UMR CNRS 5223 Ingénierie des Matériaux Polymères, Université de Lyon, 69621 Villeurbanne, France; Laboratoire Dynamique des Systèmes Mécaniques, École Militaire Polytechnique, 16046 Algiers, Algeria;* orcid.org/0000-0002-8070-490X; Phone: +213-697-005-578; Email: boumdouhanoureddine@gmail.com

Authors

Jannick Duchet-Rumeau − *UMR CNRS 5223 Ingénierie des Matériaux Polymères, Université de Lyon, 69621 Villeurbanne, France*

Jean-François Gerard − *UMR CNRS 5223 Ingénierie des Matériaux Polymères, Université de Lyon, 69621 Villeurbanne, France;* orcid.org/0000-0002-3096-2767

Djalel Eddine Tria − *Laboratoire Dynamique des Systèmes Mécaniques, École Militaire Polytechnique, 16046 Algiers, Algeria*

Amar Oukara − *Laboratoire Dynamique des Systèmes Mécaniques, École Militaire Polytechnique, 16046 Algiers, Algeria*

Complete contact information is available at: https://pubs.acs.org/10.1021/acsomega.2c06265

Author Contributions

Formal analysis, writing—original draft preparation, and funding acquisition: B.N.; resources, writing—review and editing, software, and investigation: D.R.-J.; review & editing, project administration, supervision, and visualization: G.J.-F; data curation: D.E.-T.; conceptualization and methodology: O.A. All writers approved the final manuscript.

Funding

This research was funded by the General Directorate of Scientific Research and Technological Development (DGRSDT). The Ministry of Higher Education and Scientific Research (MESRS) by Grant number #Projects PNE/2019EMP.

Notes

The authors declare no competing financial interest.

The authors state that they have no known conflicting financial interest or personal ties that might have influenced this study.

ACKNOWLEDGMENTS

The authors thank the Polymer Materials Engineering Laboratory (IMP)-UMR CNRS 5223, part of the INSA Lyon-National Institute of Applied Sciences of Lyon, for giving them all of the tools and help they needed during the training. As a result, they made their first contact with the world of research into the properties of polymers. B.N. is thankful to the Ecole Military Polytechnique (EMP) and the Ministry of Higher Education and Scientific Research (MESRS) for letting him do this job and giving him training and financial and emotional support.

REFERENCES

(1) Noureddine, B.; Zitouni, S.; Achraf, B.; Houssém, C.; Jannick, D.-R.; Jean-François, G. Development and Characterization of Tailored Polyurethane Foams for Shock Absorption. *Appl. Sci.* **2022**, *12*, 2206.

(2) Boumdouha, N.; Safidine, Z.; Boudiaf, A. Experimental Study of Loaded Foams During Free Fall Investigation and Evaluation of Microstructure. *Int. J. Adv. Manuf. Technol.* **2021**, DOI: 10.21203/rs.3.rs-792400/v1.

(3) Heiran, R.; Ghaderian, A.; Reghunadhan, A.; Sedaghati, F.; Thomas, S.; Haghighi, A. H. Glycolysis: An Efficient Route for Recycling of End of Life Polyurethane Foams. *J. Polym. Res.* **2021**, *28*, 1−19.

(4) Baghban, S. A.; Khorasani, M.; Sadeghi, G. M. M. Soundproofing Performance of Flexible Polyurethane Foams as a Fractal Object. *J. Polym. Res.* **2020**, *27*, 1−12.

(5) Dan, C. H.; Kim, Y. D.; Lee, M.; Min, B. H.; Kim, J. H. Effect of Solvent on the Properties of Thermoplastic Polyurethane/Clay Nanocomposites Prepared by Solution Mixing. *J. Appl. Polym. Sci.* **2008**, *108*, 2128−2138.

(6) Pilch-Pitera, B.; Byczyński, Ł. Study on the Thermal Behavior of New Blocked Polyisocyanates for Polyurethane Powder Coatings. *Prog. Org. Coatings* **2016**, *101*, 240−244.

(7) Kim, S. H.; Lee, M. C.; Kim, H. D.; Park, H. C.; Jeong, H. M.; Yoon, K. S.; Kim, B. K. Nanoclay Reinforced Rigid Polyurethane Foams. *J. Appl. Polym. Sci.* **2010**, *117*, 1992−1997.

(8) Harikrishnan, G.; Singh, S. N.; Kiesel, E.; Macosko, C. W. Nanodispersions of Carbon Nanofiber for Polyurethane Foaming. *Polymer* **2010**, *51*, 3349−3353.

(9) Dhasindrakrishna, K.; Pasupathy, K.; Ramakrishnan, S.; Sanjayan, J. Progress, Current Thinking and Challenges in Geopolymer Foam Concrete Technology. *Cem. Concr. Compos.* **2021**, *116*, No. 103886.

(10) Verdejo, R.; Stämpfli, R.; Alvarez-Lainez, M.; Mourad, S.; Rodriguez-Perez, M. A.; Brühwiler, P. A.; Shaffer, M. Enhanced Acoustic Damping in Flexible Polyurethane Foams Filled with Carbon Nanotubes. *Compos. Sci. Technol.* **2009**, *69*, 1564−1569.

(11) Lin, J. H.; Chuang, Y. C.; Li, T. T.; Huang, C. H.; Huang, C. L.; Chen, Y. S.; Lou, C. W. Effects of Perforation on Rigid PU Foam Plates: Acoustic and Mechanical Properties. *Materials* **2016**, *9*, 1000.

(12) Yu, T.; Jiang, F.; Cui, X.; Cao, M.; Guo, C.; Wang, Z.; Chang, Y. Properties and Mechanism of a Novel Metallic-Hollow-Spheres/Polyurethane Acoustic Composite. *J. Appl. Polym. Sci.* **2021**, *138*, 49891.

(13) Boumdouha, N.; Safidine, Z.; Boudiaf, A.; Oukara, A.; Tria, D. E.; Louar, A. In *Mechanical and Microstructural Characterization of Polyurethane Foams*, 8th Chemistry days JCh8−EMP; Military Polytechnic School (EMP): Bordj El Bahri, Algeria, 2019; p 169 DOI: 10.4000/cybergeo.24732.

(14) Zhao, Y.; Zhong, F.; Tekeei, A.; Suppes, G. J. Modeling Impact of Catalyst Loading on Polyurethane Foam Polymerization. *Appl. Catal. A Gen.* **2014**, *469*, 229−238.

(15) Li, T. T.; Liu, P.; Wang, H.; Dai, W.; Wang, J.; Wang, Z.; Shiu, B. C.; Lou, C. W.; Lin, J. H. Preparation and Characteristics of Flexible Polyurethane Foam Filled with Expanded Vermiculite Powder and Concave-Convex Structural Panel. *J. Mater. Res. Technol.* **2021**, *12*, 1288−1302.

(16) Tang, X.; Yan, X. Acoustic Energy Absorption Properties of Fibrous Materials: A Review. *Compos. Part A Appl. Sci. Manuf.* **2017**, *101*, 360−380.

(17) Ghaffari Mosanenzadeh, S.; Doutres, O.; Naguib, H. E.; Park, C. B.; Atalla, N. A Numerical Scheme for Investigating the Effect of

Bimodal Structure on Acoustic Behavior of Polylactide Foams. *Appl. Acoust.* **2015**, *88*, 75−83.
(18) Wang, J.; Xu, B.; Wang, X.; Liu, Y. A Phosphorous-Based Bi-Functional Flame Retardant for Rigid Polyurethane Foam. *Polym. Degrad. Stab.* **2021**, *186*, No. 109516.
(19) Gibson, L. J.; Ashby, M. F. *Cellular Solids: Structure and Properties*; Cambridge university press, 1999.
(20) Pagalank, P.; April, S.; Francisco, S.; Schwartz, D. S.; Evans, A. G. *Porous and Cellular Materials for Structural Applications*; MATERIALS RESEARCH SOCIETY WARRENDALE PA, 1998; Vol. *521*.
(21) Boumdouha, N.; Safidine, Z.; Boudiaf, A.; Oukara, A.; Tria, D. E.; Louar, M. A. In *Manufacture of Polyurethane Foam with a Certain Density*, The International Conference on Recent Advances in Robotics and Automation ICRARE'18; CES International Joint Conferences: Monastir − Tunisia, 2018; pp 21−30 DOI: 10.4000/cybergeo.24737.
(22) Boumdouha, N.; Safidine, Z.; Boudiaf, A.; Oukara, A.; Tria, D. E. Élaboration et Caractérisation Mécanique Des Mousses Polymères: Application Aux Projectiles Non Létaux. In *11th Days of Mechanics JM'11−EMP*; Military Polytechnic School (EMP): Bordj El Bahri: Algeria, 2011; pp 24−33 DOI: 10.4000/books.oep.332.
(23) Boumdouha, N.; Safidine, Z.; Boudiaf, A.; Djalel Eddine, T.; Oukara, A. *Élaboration et Caractérisation Mécanique Des Mousses Polyuréthanes Modifiés*, Fourth International Conference on Energy, Materials, Applied Energetics and Pollution ICEMAEP2018; Université Frères Mentouri Constantine 1: Constantine, Algeria, 2018; pp 136−142. DOI: 10.4000/cybergeo.23797.
(24) Technologies, N. *Deterring Maritime Gray Zone Aggression Ethically With Emerging Technologies*; Naval War College: Newport RI, 2019; p 298.
(25) Haar, R. J.; Iacopino, V.; Ranadive, N.; Dandu, M.; Weiser, S. D. Death, Injury and Disability from Kinetic Impact Projectiles in Crowd-Control Settings: A Systematic Review. *BMJ Open* **2017**, *7*, No. e018154.
(26) Perry, J. M. *Joint Doctrine for Nonlethal Weapons.*; Army Command and General Staff Coll Fort Leavenworth KS, 1999.
(27) de Briey, V.; de la Filolie, A.; Marinus, B. G.; Pirlot, M. Aerodynamic Characterization of a Non-Lethal Finned Projectile at Low Subsonic Velocity. *AIAA Aviation 2019 Forum* **2019**, 1−12.
(28) Yoganandan, N.; Pintar, F. A.; Zhang, J.; Gennarelli, T. A.; Beuse, N. Biomechanical Aspects of Blunt and Penentrating Head Injuries. *Solid Mech. its Appl.* **2005**, *124*, 173−184.
(29) NATO policy on non-lethal weapons. https://www.nato.int/cps/en/natohq/official_texts_27417.htm?selectedLocale=enorsimilar (accessed April 11, 2022).
(30) Gordon, S. E. Directed-Energy Non-Lethal Weapons: An Evaluation of Their Ethical Use and Potential Applications. In *Disruptive and Game Changing Technologies in Modern Warfare*; Springer, 2020; pp 93−114 DOI: 10.1007/978-3-030-28342-1.
(31) Noureddine, B.; Achraf, B.; Zitouni, S. Mechanical and Chemical Characterizations of Filled Polyurethane Foams Used for Non-Lethal Projectiles. In *10 the European Symposium on Non-Lethal Weapons EWG-NLW*; Royal Military Academy: Brussels, Belgium, 2019; p 68 DOI: 10.4000/cybergeo.24738.
(32) Orbons, J. B. J. *Non-Lethality in Reality: A Defence Technology Assessment of Its Political and Military Potential*, Universiteit van Amsterdam [Host], 2013.
(33) Papy, A.; Lemaire, E.; Robbe, C.; Nsiampa, N.; B, D.; H, P. Police Use of Non-Lethal Weapons: Analysis of Real Cases. *Hum. Factors Mech. Eng. Def. Saf.* **2019**, *3*, 9.
(34) Hatef, A.; Cooke, T. R. Winning Hearts and Minds: A Critical Analysis of Independent Media Development in Afghanistan. *J. Int. Intercult. Commun.* **2020**, *13*, 114−129.
(35) NATO Standard AEP-94. *Skin Penetration Assessment of Non-Lethal Projectiles*, 2021.
(36) NATO Standard AEP-103. *Risk Assessment of Non-Lethal Kinetic Energy Projectiles*, Vol. Ed., 3, 2021.
(37) NATO Standard AEP-98 *Precision Assessment of Non-Lethal Kinetic Energy Weapons and Ammunition* 2021.
(38) NATO Standard AEP-99. *Thorax Injury Risk Assessment of Non-Lethal Projectiles*, 2021.
(39) TAO, J.; JIANG, P.; YU, Z. On the Static Constitutive Relation of Wood With Large Deformation. *Mech. Eng.* **2000**, *22*, 25−27.
(40) Bienert, A. Command Responsibility and the Use of Force by the Police. In *The Police and International Human Rights Law*; Springer, 2018; pp 61−82 DOI: 10.1007/978-3-319-71339-7_5.
(41) ISO 2555-Plastics. *Resins in the Liquid State or as Emulsions or Dispersions-Determination of Apparent Viscosity by the Brookfield Test Method*; Geneva, Switzerland, 2018.
(42) Brethauer, S.; Antczak, A.; Balan, R.; Zielenkiewicz, T.; Studer, M. H. Steam Explosion Pretreatment of Beechwood. Part 2: Quantification of Cellulase Inhibitors and Their Effect on Avicel Hydrolysis. *Energies* **2020**, *13*, 3638.
(43) Fitzgerald, C. J.; McGavin, R. L. Blended Species Plywood (White Cypress Pine and Hoop Pine): Effect of Veneer Thickness on Susceptibility to Attack by the Subterranean Termite Coptotermes Acinaciformis. In *Bioresources*; North Carolina State University: Raleigh, 2020; pp 4655−4671 DOI: 10.15376/biores.15.3.4655-4671.
(44) Agu, H. O.; Hameed, A.; Appleby-Thomas, G. J.; Wood, D. C. The Dynamic Response of Dense 3 Dimensionally Printed Polylactic Acid. In *Journal of Dynamic Behavior of Materials*; Springer International Publishing: Cham, 2019; pp 377−386 DOI: 10.1007/s40870-019-00198-8.
(45) Curralo, A.; Queijo, L.; Rocha, J. In *Manufacturing of Lower-Limb Custom Fit Prostethics Socket Using Reverse Engineering*, Icem15: 15th International Conference on Experimental Mechanics, 2012; pp 447−448.
(46) Hsiao, S.-W.; Chuang, J.-C. A Reverse Engineering Based Approach for Product Form Design. *Des. Stud.* **2003**, *24*, 155−171.
(47) Amran, M. A. M.; Faizal, K. M.; Salleh, M. S.; Sulaiman, M. A.; Mohamad, E. Design Consideration for Design a Flat and Ring Plastics Part Using Solidworks Software. *IOP Conf. Ser. Mater. Sci. Eng.* **2015**, *100*, No. 012050.
(48) Mirrakhimova, S. R. *Integration of Information Technologies in The Educational System: Clo 3d Software in Dress Design*, Multi-discipline Proceedings of Digital Fashion Conference, 2022, Vol. 2.
(49) Haba, S. A.; Oancea, G. Design and Manufacturing Optimization of Single-Cylinder Engine Block Prototype Using CATIA Environment. In *Applied Mechanics and Materials*; Trans Tech Publications Ltd: Zurich, 2014; pp 165−170 DOI: 10.4028/www.scientific.net/AMM.474.165.
(50) Sonsalla, T.; Moore, A. L.; Radadia, A. D.; Weiss, L. Printer Orientation Effects and Performance of Novel 3-D Printable Acrylonitrile Butadiene Styrene (ABS) Composite Filaments for Thermal Enhancement. *Polym. Test.* **2019**, *80*, No. 106125.
(51) Garzon-Hernandez, S.; Garcia-Gonzalez, D.; Jérusalem, A.; Arias, A. Design of FDM 3D Printed Polymers: An Experimental-Modelling Methodology for Mechanical Property Prediction. *Mater. Des.* **2019**, *188*, No. 108414.
(52) Koffi, A.; Toubal, L.; Jin, M.; Koffi, D.; Döpper, F.; Schmidt, H.; Neuber, C. Extrusion-based 3D Printing with High-density Polyethylene Birch-fiber Composites. *J. Appl. Polym. Sci.***2022***139* 51937 DOI: 10.1002/app.51937.
(53) Di Maro, M.; Duraccio, D.; Malucelli, G.; Faga, M. G. High Density Polyethylene Composites Containing Alumina-Toughened Zirconia Particles: Mechanical and Tribological Behavior. *Composites. Part B, Engineering.* Elsevier Ltd 2021, p 108892. DOI: 10.1016/j.compositesb.2021.108892.
(54) Nsiampa, N.; Robbe, C.; Papy, A. Non-Lethal Projectile Characterisation Method: Application to 40-Mm SIR-X and Condor NT901 Projectiles. *Hum. Factors Mech. Eng. Def. Saf.* **2018**, *2*, No. 7.
(55) Nsiampa, N.; Robbe, C.; Oukara, A.; Papy, A. Comparison of Less Lethal 40mm Sponge Projectile and the 37mm Projectile for Injury Assessment on Human Thorax. In *EPJ Web Conf.*; EDP

Sciences, 2012; Vol. *26*, p 3002 DOI: 10.1051/epjconf/20122603002.
(56) Robbe, C.; Papy, A.; Nsiampa, N. Using Kinetic Energy Non-Lethal Weapons to Neutralize Low Small Slow Unmanned Aerial Vehicles. *Hum. Factors Mech. Eng. Def. Saf.* **2018**, *2*, No. 1.
(57) Wang, S.; Zhan, R. Review on Finite Element Model for Anti-Riot Kinetic Projectile Thorax Blunt Impact. *Xitong Fangzhen Xuebao/J. Syst. Simul.* **2020**, *32*, 1220−1231.
(58) 40 Mm Impact Munitions. *Tactical Response*; Hendon Publishing Company: Deerfield, 2006; p 42.
(59) Global Non-Lethal Weapons Market Analysis, Growth, Trends & Forecast 2018-2023. *M2 Presswire*; Normans Media Ltd 2018.
(60) Hubbs, K.; Klinger, D. *Impact Munitions Data Base of Use and Effects*; Ncj 204433, 2004; 1−25.
(61) Koene, B.; Id-Boufker, F.; Papy, A. Kinetic Non-Lethal Weapons. *Netherlands Annu. Rev. Mil. Stud.* **2008**, 9−24.
(62) Kapeles, J. A.; Bir, C. A. Human Effects Assessment of 40-Mm Nonlethal Impact Munitions. *Hum. Factors Mech. Eng. Def. Saf.* **2019**, *3*, 1−11.
(63) Palomar Toledano, M. Assessment of Head Injury Risk Caused by Impact Using Finite Element Models. Universitat Politècnica de València, 2020, p 211.
(64) NATO STANREC 4744 *Risk Assessment of Non-Lethal Kinetic Energy Projectiles (Appréciation Du Risque Lié Aux Projectiles Non Létaux à Énergie Cinétique)*.
(65) Clarke, J.; Coaffee, J.; Rowlands, R. *Horizon 2020 Programme Resilience Evaluation and SOTA Summary Report*; Technical report, Realising European ReSILiencE for Critical INfraStructure, 2015.
(66) Bir, C. The Evaluation of Blunt Ballistic Impacts of the Thorax. *Wayne State University*, 2000.
(67) Jacquet, J. F. In *Seuils de Concussion, Coma et Endommagements Irréversibles Lors d'un Impact Crânien Par Projectiles Cinétiques à Létalité Réduite*, 3rd congress of wound ballistics, Ecully, France, 2010.
(68) Contant, C. F.; Robertson, C. S.; Crouch, J.; Gopinath, S. P.; Narayan, R. K.; Grossman, R. G. Intracranial Pressure Waveform Indices in Transient and Refractory Intracranial Hypertension. *J. Neurosci. Methods* **1995**, *57*, 15−25.
(69) Li, Y.; Adanty, K.; Vakiel, P.; Ouellet, S.; Vette, A. H.; Raboud, D.; Dennison, C. R. Review of Mechanisms and Research Methods for Blunt Ballistic Head Injury. *J. Biomech. Eng.* **2023**, *145*, 10801.
(70) Zhou, Z.; Li, X.; Kleiven, S.; Shah, C. S.; Hardy, W. N. In *A Reanalysis of Experimental Brain Strain Data: Implication for Finite Element Head Model Validation*; SAE Technical Papers; SAE International, 2018; Vol. 2019-Novem., DOI: 10.4271/2018-22-0007.
(71) Członka, S.; Strąkowska, A. Rigid Polyurethane Foams Based on Bio-Polyol and Additionally Reinforced with Silanized and Acetylated Walnut Shells for the Synthesis of Environmentally Friendly Insulating Materials. *Materials* **2020**, *13*, 3245.
(72) Ma, X.; von Seggern, H.; Sessler, G. M.; Zhukov, S.; Ben Dali, O.; Kupnik, M.; Zhang, X. High Performance Fluorinated Polyethylene Propylene Ferroelectrets with an Air-Filled Parallel-Tunnel Structure. *Smart Mater. Struct.* **2021**, *30*, No. 015002.
(73) Boumdouha, N.; Zitouni, S.; Achraf, B. A New Study of Dynamic Mechanical Analysis and the Microstructure of Polyurethane Foams Filled. *Turkish J. Chem.* **2022**, *46*, 814−834.
(74) Boumdouha, N.; Safidine, Z.; Boudiaf, A.; Duchet-Rumeau, J.; Gerard, J.-F. Experimental Study of the Dynamic Behaviour of Loaded Polyurethane Foam Free Fall Investigation and Evaluation of Microstructure. *Int. J. Adv. Manuf. Technol.* **2022**, *120*, 3365−3381.
(75) Thota, N.; Epaarachchi, J.; Lau, K. T. Evaluation of the Performance of Three Elastomers for Non-Lethal Projectile Applications. In *EPJ Web Conf.*; EDP Sciences, 2015; Vol. *94*, p 3002 DOI: 10.1051/epjconf/20159403002.
(76) Gibson, L. J.; Ashby, M. F. The Mechanics of Foams: Basic Results. In *Cellular Solids*; Cambridge University Press, 2014; pp 175−234 DOI: 10.1017/cbo9781139878326.007.
(77) Cimavilla-Román, P.; Pérez-Tamarit, S.; Santiago-Calvo, M.; Rodríguez-Pérez, M. Á. Influence of Silica Aerogel Particles on the Foaming Process and Cellular Structure of Rigid Polyurethane Foams. *Eur. Polym. J.* **2020**, *135*, No. 109884.
(78) Abdollahi Baghban, S.; Khorasani, M.; Mir Mohamad Sadeghi, G. Soundproofing Flexible Polyurethane Foams: Effect of Chemical Structure of Chain Extenders on Micro-Phase Separation and Acoustic Damping. *J. Cell. Plast.* **2020**, *56*, 167−185.
(79) Li, Z.; Han, X.; Ge, H.; Ma, C. A Semi-Automatic Method of Generating Subject-Specific Pediatric Head Finite Element Models for Impact Dynamic Responses to Head Injury. *J. Mech. Behav. Biomed. Mater.* **2016**, *60*, 557−567.
(80) Chen, C.; Zhao, F.; Bao, H.; Zhuang, H. Research on Modeling and Simulation of Head Injury Assessment Based on LSDYNA Software Technology. *J. Phys.: Conf. Series; IOP Publ.* **2021**, *2030*, 12054.
(81) Tierney, G. Concussion Biomechanics, Head Acceleration Exposure and Brain Injury Criteria in Sport: A Review. *Sport. Biomech.* **2022**, 1−29.
(82) Boumdouha, N.; Safidine, Z.; Boudiaf, A. Preparation of Nonlethal Projectiles by Polyurethane Foam with the Dynamic and Microscopic Characterization for Risk Assessment and Management. *ACS Omega* **2022**, *7*, 16211−16221.

https://doi.org/10.1021/acsomega.2c06265
ACS Omega 2022, 7, 47129−47147